



**HAL**  
open science

# Griffiths phase and critical behavior of the 2D Potts models with long-range correlated disorder

Christophe Chatelain

► **To cite this version:**

Christophe Chatelain. Griffiths phase and critical behavior of the 2D Potts models with long-range correlated disorder. *Physical Review E: Statistical, Nonlinear, and Soft Matter Physics*, 2014, 89, pp.032105. 10.1103/PhysRevE.89.032105 . hal-00850126v2

**HAL Id: hal-00850126**

**<https://hal.science/hal-00850126v2>**

Submitted on 22 Feb 2014

**HAL** is a multi-disciplinary open access archive for the deposit and dissemination of scientific research documents, whether they are published or not. The documents may come from teaching and research institutions in France or abroad, or from public or private research centers.

L'archive ouverte pluridisciplinaire **HAL**, est destinée au dépôt et à la diffusion de documents scientifiques de niveau recherche, publiés ou non, émanant des établissements d'enseignement et de recherche français ou étrangers, des laboratoires publics ou privés.

# Griffiths phase and critical behavior of the 2D Potts models with long-range correlated disorder

Christophe Chatelain

*Groupe de Physique Statistique, Département P2M,  
Institut Jean Lamour (CNRS UMR 7198), Université de Lorraine, France*

(Dated: February 22, 2014)

The  $q$ -state Potts model with a long-range correlated disorder is studied by means of large-scale Monte Carlo simulations for  $q = 2, 4, 8$  and  $16$ . Evidence is given of the existence of a Griffiths phase, where the thermodynamic quantities display an algebraic Finite-Size Scaling, in a finite range of temperatures. The critical exponents are shown to depend on both the temperature and the exponent of the algebraic decay of disorder correlations, but not on the number of states of the Potts model. The mechanism leading to the violation of hyperscaling relations is observed in the entire Griffiths phase.

PACS numbers: PACS numbers: 64.60.De, 05.50.+q, 05.70.Jk, 05.10.Ln

## I. INTRODUCTION

It is well known that the presence of impurities can greatly affect the properties of a physical system, especially when the latter undergoes a phase transition. In the following, the case of frozen impurities, i.e. quenched disorder, coupled to the energy density of the system is considered. It is assumed that no frustration is induced by randomness. With these assumptions, Harris analyzed the conditions for a change of critical behavior at a second-order phase transition upon the introduction of disorder [1]. In the language of Renormalization Group (RG), disorder is a relevant perturbation when its fluctuations in a finite domain grow faster than the fluctuations of the energy, or equivalently, when the specific heat exponent  $\alpha$  of the pure model is positive. On the theoretical side, the  $q$ -state Potts model provides a useful and simple toy model to study the influence of disorder. In two dimensions, the pure model undergoes a second-order phase transition when  $q \leq 4$  with a  $q$ -dependent universality class. Upon the introduction of quenched disorder, the critical behavior is governed by a new  $q$ -dependent RG fixed point when  $2 < q \leq 4$ . A good agreement between numerical calculations [2] and RG series expansions [3] of the critical exponents has been achieved. In the case  $q = 2$ , equivalent to the Ising model, disorder is a marginally irrelevant perturbation and the critical behavior is only modified by multiplicative logarithmic corrections [4]. In the three-dimensional case, only the Ising model undergoes a second-order phase transition. As predicted by the Harris criterion, a new critical behavior is found by RG studies and observed numerically [5].

When the pure system undergoes a first-order phase transition, the introduction of disorder softens the energy jump and reduces the latent heat [6]. For a strong enough disorder, a continuous phase transition can be induced. In two dimensions, an infinitesimal amount of disorder is sufficient to induce a second order phase transition [7, 8]. This rigorously-proved

statement was first tested in the case of the 8-state Potts model [9]. In the entire regime  $q > 4$ , where a first-order phase transition is undergone by the pure Potts model, a continuous transition is induced with a  $q$ -dependent critical behavior [10]. In three dimensions, the softening of the transition was observed numerically for the  $q = 3$  [11] and  $q = 4$  [12] Potts models, as well as in the limit  $q \rightarrow +\infty$  [13]. For weak disorder, the transition remains discontinuous, while at strong disorder, it becomes continuous.

It was implicitly assumed in the above discussion that the disorder was uncorrelated. This may not be the case anymore if the impurities interact and were given enough time to equilibrate. This situation may be encountered with charged impurities. At a second-order phase transition, long-range correlated disorder leads to a critical behavior that can be distinct from the case of short-range or uncorrelated disorder. Weinrib and Halperin studied by RG the  $n$ -component  $\phi^4$ -model in dimension  $d$  with a correlated disorder decaying algebraically with an exponent  $a$  [14]. In the same spirit as the Harris criterion, such a long-range correlated disorder is shown to be relevant when the correlation exponent  $\nu$  of the pure model satisfies the inequality  $\nu < 2/a$ . Interestingly, disorder is a marginally irrelevant perturbation at the new long-range random fixed point, which means that  $\nu = 2/a$ . This relation was proved to be exact at all orders in perturbation [15] and was later confirmed by Monte Carlo simulations of the 3D Ising model [16] and an explicit RG calculation of the 2D Ising model [17].

Weinrib and Halperin calculation is based on the assumption that disorder correlations are isotropic and that  $n$ -point disorder cumulants are irrelevant for  $n > 2$ . Anisotropically correlated disorder is therefore out of its range of validity. The latter has attracted a lot of attention since the introduction of the celebrated McCoy-Wu model [19], which corresponds to an Ising model with randomly distributed couplings  $J_1$  and  $J_2$  in one direction and infinitely correlated in the second

direction of the square lattice [19]. While planar defects lead to a smearing of the transition of the 3D Ising model [18], the phase transition of this 2D Ising model with parallel linear defects remains sharp. Exploiting the mapping to the Ising quantum chain in a transverse field, the critical exponents were determined exactly:  $\beta = (3 - \sqrt{5})/2$  and  $\nu = 2$  [20]. Because of the layered structure, the anisotropy exponent  $z$  is infinite. The isotropy can be restored by an appropriate superposition of two McCoy-Wu models oriented in two different directions. A different magnetic critical behavior is then observed [22]. When algebraically decaying disorder correlations are introduced in the transverse direction of the McCoy-Wu model, the Weinrib-Halperin law  $\nu = 2/a$ , where  $a$  is the disorder correlation exponent, is recovered [21]. Interestingly, the critical behavior of the Potts model with uncorrelated homogeneous disorder was conjectured to be described by an isotropic version of the McCoy-Wu-Fisher fixed point in the limit  $q \rightarrow +\infty$  [23].

The McCoy-Wu model is easily extended to  $q$ -state Potts spins. In the regime  $q \leq 4$ , the critical behavior was proved to be independent of the number of states  $q$  and therefore identical to that of the original McCoy-Wu model [26]. Numerical calculations showed that the first-order phase transition of the Potts model with  $q > 4$  is completely rounded, like in the case of homogeneous disorder, but, in contrast to homogeneous disorder, the critical behavior induced by disorder is independent of  $q$  and therefore described by the infinite-disorder McCoy-Wu-Fisher fixed point [27]. Different arrangements of correlated couplings were also studied. An aperiodic sequence of couplings  $J_1$  and  $J_2$  in one direction, infinitely correlated in the second direction of a square lattice, also provokes the rounding of the first-order phase transition of the Potts model when the wandering exponent of the sequence is sufficiently large [28]. However, in contrast to the McCoy-Wu model, the induced critical behavior depends on the number of states  $q$ .

The McCoy-Wu model is the first model where a Griffiths phase was observed [24]. In a finite range of temperatures around the critical point, the free energy is a singular function of the magnetic field. Consequently, the magnetization is also singular and the magnetic susceptibility diverges for all temperatures in the Griffiths phase. The Griffiths phase should also be present in the aforementioned Potts models with isotropic disorder but it is believed to be too weak to be observed numerically. In the following, the mechanism leading to such a Griffiths phase is briefly discussed in the case of a binary distribution of strong and weak couplings, say  $J_1$  and  $J_2$  respectively. The critical temperature  $T_c$  of the random system is expected to lie between the critical temperatures  $T_1$  and  $T_2$  of homogeneous systems with only strong or weak couplings. A rough estimate of these temperatures is given by

$k_B T_1 \simeq J_1$  and  $k_B T_2 \simeq J_2$ . In the paramagnetic phase  $T > T_c$ , the Griffiths phase is caused by the existence of rare macroscopic regions with a high concentration of strong couplings  $J_1$ . While the rest of the system is still not ordered, they can order independently for all temperatures  $T_c \leq T < T_1$  [25]. Because these regions are macroscopic, they cannot be easily flipped by local Monte Carlo algorithms. The spin-spin autocorrelation functions can be shown to decay much slower than the expected exponential decay in a paramagnetic phase. Below the critical temperature, the Griffiths phase is caused by the existence of ordered domains isolated of the rest of the system by a high concentration of weak bonds at its frontiers. This mechanism is therefore effective for temperatures  $T_2 \leq T \leq T_c$ .

Recently, we have studied the 2D 8-state Potts model with an isotropic correlated non-Gaussian disorder [29]. Such a disorder was obtained by simulating an Ashkin-Teller model on a critical line of its phase diagram. To each independent spin configuration is assigned a coupling configuration for the Potts model. We have shown by Monte Carlo simulations that the first-order phase transition of the 8-state Potts model is rounded. Disorder fluctuations are large and cause the violation of the hyperscaling relation, in the same way as in the 3D random-field Ising model, even though no frustration is present. In this work, we show by means of large-scale Monte Carlo simulations that this behavior is actually observed in a finite range of temperatures and for all numbers of states  $q$  of the Potts model. The equivalent of 25 years on a single CPU was used. The paper is organized as follows. Details about the model and the simulations are given in section II. The phase diagram is discussed and evidences are given of the existence of a Griffiths phase in section III. The critical behavior in this Griffiths phase is then presented in section IV. Non self-averaging properties and hyperscaling violation are finally discussed in section V. A conclusion follows.

## II. MODELS AND NUMERICAL DETAILS

### A. The Potts model

The Potts model is a generalization of the Ising model where the classical degrees of freedom, called spins, lie on the nodes of a lattice and can take  $q$  possible values, for example  $\{0, 1, \dots, q-1\}$ . In the following,  $\sigma_i$  denotes the spin lying on the  $i$ -th node of the lattice. Spins are assumed to interact only if they are on nearest-neighbor sites. The Potts Hamiltonian is defined as [30]

$$H = - \sum_{(i,j)} J \delta_{\sigma_i, \sigma_j} \quad (1)$$

where the sum is restricted to pairs of nearest neighbors  $i$  and  $j$  of the lattice. The Ising model is recovered in

the case  $q = 2$ . Note that the Fortuin-Kasteleyn representation of the Potts model allows for a generalization to non-integer values of  $q$  [31]. As mentioned in the introduction, the Potts model undergoes a phase transition which is of first order for  $q > q_c$  and continuous for  $q \leq q_c$ . The value  $q_c$  depends on the number of dimensions of the lattice. In the two-dimensional case,  $q_c = 4$  and duality arguments based on the Fortuin-Kasteleyn representation show that the transition temperature is given by

$$(e^{\beta J} - 1) = \sqrt{q} \quad (2)$$

where  $\beta = 1/k_B T$ . The Potts Hamiltonian (1) is unchanged under the global circular shift  $\sigma_i \rightarrow \sigma_i = (\sigma_i + 1) \bmod q$ . This  $\mathbb{Z}_q$ -symmetry is broken in the low-temperature phase, where a majority of spins can be found in the same state. The order parameter  $m$ , called magnetization, can therefore be defined as

$$m = \frac{q\rho_{\max.} - 1}{q - 1} \quad (3)$$

where  $\rho_{\max.}$  is the fraction of spins in the majority state.

In the following, we are interested in the influence of quenched disorder coupled to the energy density. On each lattice edge  $(i, j)$ , joining the two neighboring sites  $i$  and  $j$ , the exchange coupling  $J$  appearing in the Hamiltonian (1) is replaced by a random variable  $J_{ij}$ :

$$H = - \sum_{(i,j)} J_{ij} \delta_{\sigma_i, \sigma_j} \quad (4)$$

The calculation of the thermodynamic quantities requires an average over both the thermal fluctuations and the coupling configurations:

$$\overline{\langle X \rangle} = \sum_{\{J_{ij}\}} \wp(\{J_{ij}\}) \left[ \frac{1}{\mathcal{Z}[J_{ij}]} \sum_{\{\sigma_i\}} e^{-\beta H[\sigma_i, J_{ij}]} \right]. \quad (5)$$

The average over thermal fluctuations is denoted by brackets  $\langle m \rangle$  in the case of magnetization. The over line corresponds to the average over the probability distribution  $\wp(\{J_{ij}\})$  of the random couplings  $J_{ij}$ . Duality arguments can be extended to the random case. Consider a coupling configuration  $\{J_{ij}\}$ . The image of this configuration under the duality transformation is a new coupling configuration  $\{J_{ij}^*\}$  where the dual bonds are defined by [33]

$$(e^{\beta J} - 1)(e^{\beta J^*} - 1) = q. \quad (6)$$

The singular part of the average free energy density is unchanged if the self-duality condition

$$\wp(\{J_{ij}\}) = \wp(\{J_{ij}^*\}) \quad (7)$$

on the probability distribution of the random couplings is satisfied. In numerical studies, the binary distribution

$$\wp(J_{ij}) = \frac{1}{2} \delta(J_{ij} - J_1) + \frac{1}{2} \delta(J_{ij} - J_2) \quad (8)$$

is usually the simplest choice. The critical line is therefore given by the self-duality condition

$$J_1 = J_2^* \Leftrightarrow (e^{\beta_c J_1} - 1)(e^{\beta_c J_2} - 1) = q. \quad (9)$$

Note that the self-duality condition (7) is a constraint on the probability distribution  $\wp(\{J_{ij}\})$ . In the case of the binary distribution (8), it does not impose the strict equality of the numbers of couplings  $J_1$  and  $J_2$  in each disorder realization, though these numbers will converge towards the same value in the thermodynamic limit. In the framework of RG, the fluctuations of the numbers of couplings  $J_1$  and  $J_2$  in a coupling configuration have been moreover shown to be an irrelevant perturbation at the random fixed point [32]. The self-duality condition (7) is very general and still holds in the case of correlated disorder.

## B. The auxiliary Ashkin-Teller model

In order to generate the coupling configurations  $\{J_{ij}\}$  of the Potts model, an auxiliary isotropic Ashkin-Teller model is simulated. This model corresponds to two Ising models locally coupled by their energy density and is defined by the Hamiltonian [35]

$$-\beta H^{\text{AT}} = \sum_{(i,j)} [J^{\text{AT}} \sigma_i \sigma_j + J^{\text{AT}} \tau_i \tau_j + K^{\text{AT}} \sigma_i \sigma_j \tau_i \tau_j]. \quad (10)$$

This Hamiltonian is invariant under the reversal of all spins  $\sigma_i$ , all spins  $\tau_i$  or both  $\sigma_i$  and  $\tau_i$ . Two order parameters can be defined: magnetization  $M = \langle |\sum_i \sigma_i| \rangle$  and polarization  $P = \langle |\sum_i \sigma_i \tau_i| \rangle$ . The phase diagram of the Ashkin-Teller model presents several lines separating a paramagnetic phase ( $M = P = 0$ ), a Baxter phase where all spins are in the same state ( $M, P \neq 0$ ) and a phase where each Ising replica is disordered but there exists order between them ( $M = 0, P \neq 0$ ). The line separating the paramagnetic and Baxter phases is given by self-duality arguments [36]:

$$e^{-2K} = \sinh 2J. \quad (11)$$

The critical exponents along this line were obtained through the conjecture of a mapping [37] of the Ashkin-Teller model onto an eight-vertex model exactly solved by Baxter. In terms of the parameter  $y \in [0, 4/3]$  of the eight-vertex model and related to the couplings along the line by

$$\cos \frac{\pi y}{2} = \frac{1}{2} [e^{4K} - 1], \quad (12)$$

these critical exponents read

$$\beta_{\sigma}^{\text{AT}} = \frac{2 - y}{24 - 16y}, \quad \beta_{\sigma\tau}^{\text{AT}} = \frac{1}{12 - 8y}, \quad \nu^{\text{AT}} = \frac{2 - y}{3 - 2y}. \quad (13)$$

Note that  $\beta_{\sigma}^{\text{AT}}/\nu^{\text{AT}} = 1/8$  is constant while  $\beta_{\sigma\tau}^{\text{AT}}/\nu^{\text{AT}}$  varies along the self-dual line. Therefore, polarization-polarization correlation functions decay algebraically

$$\langle \sigma_i \tau_i \sigma_j \tau_j \rangle \sim |\vec{r}_i - \vec{r}_j|^{-a} \quad (14)$$

with an exponent

$$a = 2\beta_{\sigma\tau}^{\text{AT}}/\nu^{\text{AT}} = \frac{1}{4 - 2y} \quad (15)$$

that can be tuned by moving along the critical line. In order to construct correlated coupling configurations for the Potts model, a set of typical spin configurations of the Ashkin-Teller model at different points of the self-dual line are first generated by Monte Carlo simulation. We used the cluster algorithm proposed by Wiseman and Domany [38].

To each spin configuration is then associated a coupling configuration of the Potts model by

$$J_{ij} = \frac{J_1 + J_2}{2} + \frac{J_1 - J_2}{2} \sigma_i \tau_i \quad (16)$$

where the site  $j$  is located after the site  $i$  on the lattice, i.e. on its right or below. At each site, two couplings are therefore always identical, one being horizontal and the other vertical. Because of this construction, disorder correlations  $(J_{ij} - \bar{J})(J_{kl} - \bar{J})$  decay algebraically, like the polarization, with an exponent  $a$  that can be tuned. We have considered the six values  $y \in \{0, 0.25, 0.50, 0.75, 1, 1.25\}$  corresponding to the exponents  $a \simeq 0.25, 0.286, 0.333, 0.4, 0.5$  and  $0.667$ . The two couplings  $J_1$  and  $J_2$  are chosen to be related by

$$(e^{J_1} - 1)(e^{J_2} - 1) = q \quad (17)$$

corresponding to the self-duality condition (9) when  $\beta = 1/k_B T = 1$ , i.e. the self-dual point is located at  $\beta_c = 1$ . At this temperature,  $J_1$  is indeed equal to  $J_2^*$ . Because of the construction (16), the duality transformation  $J_{ij} \rightarrow J_{ij}^*$  is equivalent to a global reversal  $\sigma_i \tau_i \rightarrow -\sigma_i \tau_i$  of the local polarization of the auxiliary Ashkin-Teller model. Since the Hamiltonian of the latter is unchanged under this transformation, the Boltzmann weight is unaffected. In terms of coupling configurations, this leads to the self-duality condition (7).

On average, the total number of strong and weak couplings are equal. However, in a finite system, these numbers fluctuate from sample to sample. According to the central limit theorem, these fluctuations vanish as  $1/\sqrt{N} \sim 1/L$ , where  $N = L^2$  is the total number of sites, in the case of uncorrelated disorder. For the correlated disorder introduced above, these fluctuations scale with the lattice size as the polarization of the Ashkin-Teller model, i.e. as  $L^{-\beta_{\sigma\tau}^{\text{AT}}/\nu^{\text{AT}}} = L^{-a/2}$ . Since the values  $a \simeq 0.25, 0.286, 0.333, 0.4, 0.5$  and  $0.667$  are considered, fluctuations decay slower than in the case of uncorrelated disorder. Moreover, for the lattice sizes

considered in this work, these fluctuations are much smaller for uncorrelated disorder than for correlated one. For  $L = 256$  and  $y = 0.75$ , an average polarization  $|\overline{p}| \simeq 0.343(1)$  is measured while for uncorrelated disorder, the equivalent quantity reconstructed from the couplings is  $|\overline{p}| \simeq 0.0499(1)$  for  $L = 16$  already.

Note that, in the following, this disorder will be referred to as correlated disorder to distinguish it from uncorrelated disorder. However, it is important to keep in mind that, as described above, it was obtained using a very particular construction and does not display the same properties as the correlated disorder considered by Weinrib and Halperin. In the latter, disorder was indeed distributed according to a Gaussian probability distribution so that  $2n$ -point correlation functions are related to two-point correlations by the Wick theorem. This is not the case for the Ashkin-Teller model and, therefore, for the couplings that are generated from the typical spin configurations of this model.

### III. TEMPERATURE DEPENDENCE

In this section, the temperature dependence of the average thermodynamic quantities is investigated to determine the phase diagram of the model. Note that the temperature affects only the Potts model and not the auxiliary Ashkin-Teller model used to construct the coupling configurations. Disorder correlations decay algebraically independently of the temperature. Two numbers of Potts states,  $q = 2$  (equivalent to the Ising model) and  $q = 8$ , are considered. As mentioned in the introduction, the former undergoes a second-order phase transition in the absence of disorder while the latter displays a discontinuous transition. Monte Carlo simulations with the Swendsen-Wang cluster algorithm [34] were performed for the lattice sizes  $L = 32, 48, 64$  and  $96$ . The exponent of the algebraic decay of the disorder correlations was fixed to  $a = 0.4$ , which corresponds to a parameter  $y = 0.75$  for the auxiliary Ashkin-Teller model. For comparison, the case of an uncorrelated disorder is also considered and presented in an inset in each figure. The thermodynamic quantities were averaged over 14563 disorder configurations for  $L = 96$ , 32768 for  $L = 64$ , 58254 for  $L = 48$  and 131072 for  $L = 32$ . For each disorder configuration, 2000 Monte Carlo iterations were performed to estimate the thermal averages. The autocorrelation time depends on the temperature but never exceeds the values  $\tau \simeq 2$  for the Ising model and  $\tau \simeq 8$  for the 8-state Potts model. The case of the Ising model is first discussed.

#### A. Ising model

As can be observed on Fig. 1, the magnetization curve of the Ising model with correlated disorder

is not typical. Instead of the usual single abrupt variation of magnetization, two such variations are seen. Between the paramagnetic and ferromagnetic phases, an intermediate region of slow variation is present. This behavior is remarkably different from the case of uncorrelated disorder shown in the inset. With correlated disorder, the magnetization displays a strong lattice-size dependence in the intermediate regime, similar to what is observed in the paramagnetic phase. As will be more extensively discussed in the next section, this behavior is algebraic. It is tempting to associate the boundaries of this intermediate regime to the two temperature scales introduced by the two Potts couplings  $J_1$  and  $J_2$ . In the case presented here, these two couplings are solutions of the self-duality condition (17) with  $r = J_2/J_1 = 3$ . Numerically,  $J_1 \simeq 0.4812$  and  $J_2 \simeq 1.4436$ . Neighboring spins linked by strong couplings  $J_2$  are preferably in the same state for inverse temperatures  $\beta = \frac{1}{k_B T} \lesssim \frac{1}{J_2} \simeq 0.6927$ . As can be seen on Fig. 1, a quick variation of magnetization is indeed observed around this temperature. Weak couplings introduce a second inverse temperature scale  $\beta = \frac{1}{J_1} \simeq 2.079$  which is, in contrast, further from the second fast variation of magnetization which occurs already around  $\beta \simeq 1.50$ .

The magnetic susceptibility, plotted in Fig. 2, displays two peaks, in contrast to the single peak observed in the case of uncorrelated disorder (see the inset of Fig. 2). These two peaks appear at temperatures similar to those for which an abrupt variation of magnetization was observed. The magnetic susceptibility diverges algebraically with the lattice size for all temperatures in the region between the two peaks (note the use of a logarithmic scale for the  $y$ -axis on the figure). The critical exponent associated to this divergence will be discussed in the next section. We are therefore in presence of a Griffiths phase, like in the McCoy-Wu model. As mentioned in the introduction, the occurrence of such a Griffiths phase in the McCoy-Wu model was explained by the existence of exponentially rare macroscopic regions that can order independently of the rest of the system. The susceptibility of each disorder configuration is plotted on Fig. 3 versus the polarization density  $p = \langle \sigma_i \tau_i \rangle$  of the auxiliary Ashkin-Teller model. By construction (16),  $p$  depends linearly on the concentration of strong couplings  $J_2$ . The value  $p = -1$  corresponds to the configuration with only weak couplings  $J_1$  while all couplings are strong when  $p = +1$ . As can be observed on Fig. 3, the largest susceptibility is observed for disorder configurations with different polarizations as the temperature is increased. In the paramagnetic phase (left of Fig. 3), the largest susceptibility is due to configurations with a high concentration of strong couplings. To understand this behavior, consider the two configurations with identical couplings, either  $J_1$  or  $J_2$ . The system is expected to behave like a pure Potts model. Therefore, at large temperature  $\beta J_1 < \beta J_2 < \beta_c$ ,

a lattice of strong couplings  $J_2$  is closer to the transition point than a configuration with mainly weak couplings  $J_1$ . Analogously, in the ferromagnetic phase (right of Fig. 3), the average susceptibility is dominated by disorder configurations with small concentrations of strong couplings. In the Griffiths phase (center of Fig. 3), the main contribution comes from disorder configurations with a slightly negative polarization, i.e. a number of strong couplings slightly below the number of weak ones. In such configurations, different clusters of weak or strong couplings are typically observed. The average magnetization is around 0.4, which means that the largest cluster of strong couplings occupies at most 40% of the sites. There is therefore plenty of space left for other clusters, possibly macroscopic too. Note that the width of the bunch of points in Fig. 3 increases in the Griffiths phase: at fixed polarization, some disorder configurations lead to susceptibilities  $\sim 60$  times larger than others. In the case of uncorrelated disorder, we did not find any temperature, among those studied, for which the plot of susceptibilities versus polarization looks like Fig. 3 in the Griffiths phase.

In the case of uncorrelated disorder, it is well known that sample-to-sample fluctuations increase drastically with the lattice size at the critical point. One consequence is the lack of self-averaging of thermodynamic quantities when randomness is a relevant perturbation. Averages are then dominated by rare, rather than typical, events. In the (uncorrelated) random Potts model, self-averaging is broken only at the critical point. Below and above, self-averaging is restored in the thermodynamic limit. In the correlated case, magnetization is a non self-averaging quantity in the whole Griffiths phase. Following Wiseman and Domany [39], the lack of self-averaging of magnetization is measured by comparing the variance with the average:

$$R_m = \frac{\overline{\langle m \rangle^2} - \langle m \rangle^2}{\langle m \rangle^2}. \quad (18)$$

This ratio is expected to go to a non-vanishing limit in the thermodynamic limit when self-averaging is not satisfied. As can be seen on Fig. 4, this is the case in the Griffiths phase. The value taken by  $R_m$  in the thermodynamic limit is expected to be universal [40]. While no dependence on the strength of disorder is observed,  $R_m$  is however not constant in the Griffiths phase but depends on the temperature. This implies that the critical behavior in the Griffiths phase is not described by a single universality class. We will come back to that point in next section. The case of the Ising model with uncorrelated disorder is very different: as shown in the inset of Fig. 4, the ratio  $R_m$  displays a thinner and thinner peak whose maximum is close to the critical temperature. The maximum of this peak is expected to vanish in the thermodynamic limit since randomness is irrelevant. A similar ratio  $R_\chi$  for the susceptibility

was indeed shown to decrease slowly as  $1/\ln L$  [41]. Such a slow decay is also observed in the inset of Fig. 4, though the maxima are still compatible within error bars.

Like the magnetic susceptibility, the specific heat displays two peaks (Fig. 5). However, it depends only weakly on the lattice size. At the peaks, the data are compatible for all lattice sizes. In between, a small increase of the specific heat with the lattice size is observed. Note that the scale of the  $y$ -axis is only linear and not logarithmic, so the evolution with the lattice size is extremely slow. When plotted versus the polarization, the specific heat of the different disorder configurations presents a much more weakly bended shape than the magnetic susceptibility. The largest and smallest specific heats differ at most by a factor  $\sim 2$ . The computation of the ratio

$$R_e = \frac{\overline{\langle e \rangle^2} - \overline{\langle e \rangle}^2}{\overline{\langle e \rangle}^2} \quad (19)$$

reveals that energy is a self-averaging quantity at all temperatures, including the critical temperature. This is also the case for uncorrelated disorder. To conclude, no evidence of Griffiths phase is found with thermal quantities, in contrast to the magnetic sector.

Finally, we note that the autocorrelation time  $\tau$  also displays two peaks, whereas only one peak is observed in the absence of disorder correlation. These two peaks are found at the same locations as for the magnetic susceptibility or specific heat. The autocorrelation time evolves slowly with the lattice size, which means that the autocorrelation exponent  $z$  is close to zero.

### B. $q = 8$ Potts model

The 8-state Potts model with correlated disorder displays a behavior very similar to that of the Ising model presented above. Like in the case of uncorrelated disorder, the fact that the pure system undergoes a first-order phase transition does not lead to any significant difference. The magnetization curve displays two abrupt variations (Fig. 6). The location of these fast variations coincides with the two peaks of the magnetic susceptibility (Fig. 7). For the 8-state Potts model, a stronger disorder  $r = 7.5$  was considered, which means that  $J_1 \simeq 0.3855$  and  $J_2 \simeq 2.891$ . In contrast to the Ising case, the first temperature scale  $\beta = \frac{1}{k_B T} = \frac{1}{J_2} \simeq 0.3459$  is significantly smaller than the location of the first peak (around 0.50). The second temperature scale  $\frac{1}{J_1} \simeq 2.594$  is smaller than the location of the second peak. When plotted versus the polarization of the auxiliary Ashkin-Teller model, the susceptibilities of the different disorder configurations are very similar to those of Fig. 3. In the Griffiths phase, the largest susceptibilities are again observed at a small negative polarization ( $\simeq -0.05$ )

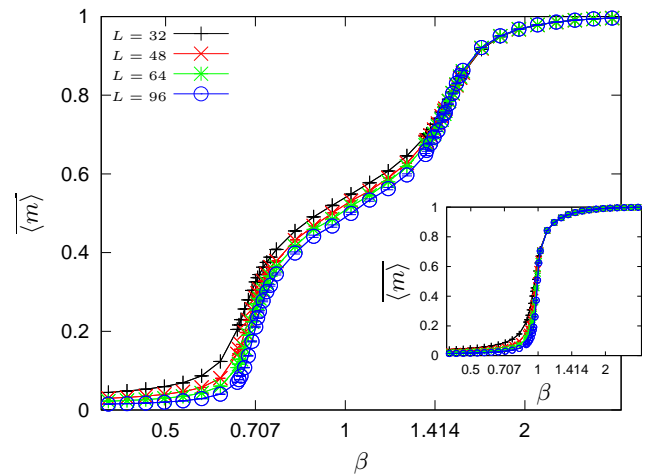


FIG. 1. (Color online) Average magnetization of the Ising model ( $q = 2$ ), with a disorder strength  $r = 3$  and a correlation exponent  $a = 0.4$  ( $y = 0.75$ ), versus the inverse temperature  $\beta = 1/k_B T$ . The different curves correspond to different lattice sizes ( $L = 32, 48, 64$  and  $96$ ). In the inset, the magnetization curve in the case of uncorrelated disorder is plotted.

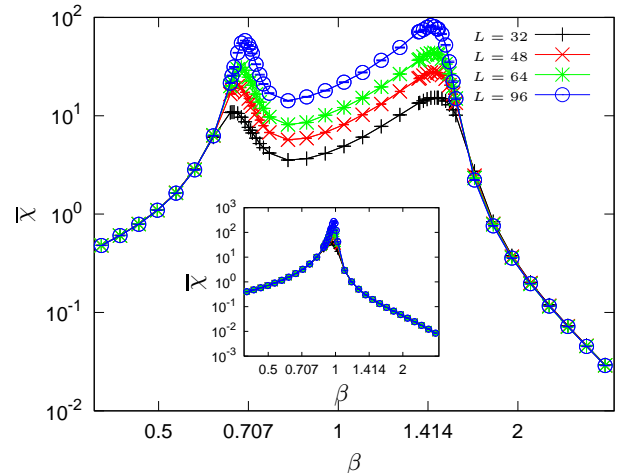


FIG. 2. (Color online) Average susceptibility of the Ising model ( $q = 2$ ), with a disorder strength  $r = 3$  and a correlation exponent  $a = 0.4$  ( $y = 0.75$ ), versus the inverse temperature  $\beta = 1/k_B T$ . The different curves correspond to different lattice sizes ( $L = 32, 48, 64$  and  $96$ ). In the inset, the average susceptibility in the case of uncorrelated disorder is plotted.

i.e. for disorder configurations with a slightly smaller number of strong couplings than weak ones. The main difference with the Ising model is a much larger spreading of the bunch of points. The ratio between the largest and the smallest susceptibilities at fixed polarization is  $\sim 330$ . The ratio Eq. 18 is plotted on Fig. 8 in the case of the 8-state Potts model. Like in the Ising case, magnetization is not self-averaging in the Griffiths phase.

The specific heat does not display such properties.

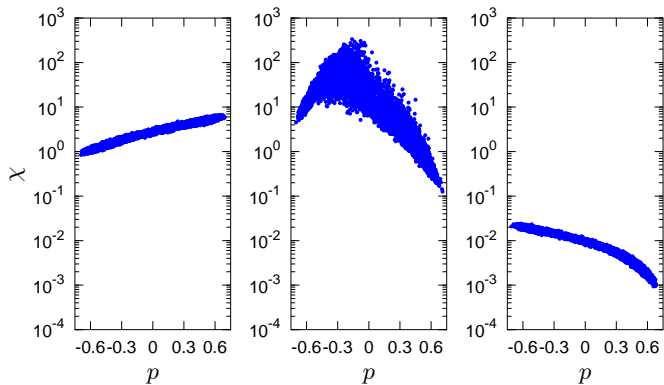


FIG. 3. (Color online) Susceptibility  $\chi$  of the Ising model with correlated disorder ( $a = 0.4$ ,  $r = 3$ ) versus the polarization density  $p$  of the disorder realization for  $\beta \simeq 0.535$  (left), 1.022 (center) and 2.801 (right). Each point corresponds to a different disorder realization. The lattice size is  $L = 96$ .

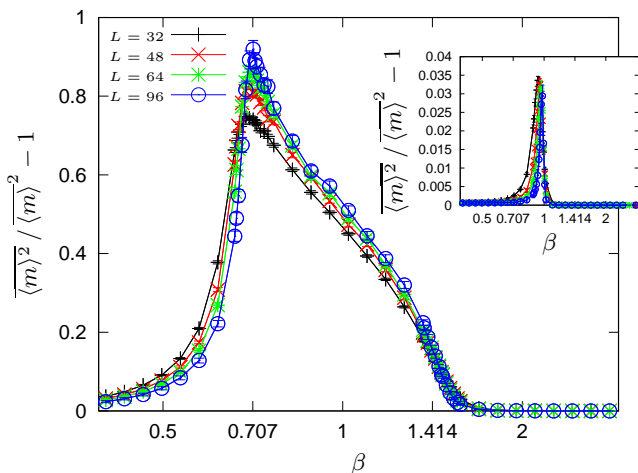


FIG. 4. (Color online) Self-averaging ratio  $R_m$  of magnetization of the Ising model ( $q = 2$ ), with a disorder strength  $r = 3$  and a correlation exponent  $a = 0.4$  ( $y = 0.75$ ), versus the inverse temperature  $\beta = 1/k_B T$ . In the inset, ratio in the case of uncorrelated disorder.

Even though two peaks can be observed (Fig. 9), the specific heat is essentially size-independent, even at and between the two peaks. The ratio Eq. 19 vanishes at all temperatures which implies that energy is a self-averaging quantity.

Like in the Ising case, the autocorrelation time also displays two peaks located at the same temperatures as for the magnetic susceptibility or the specific heat. The peaks are more pronounced than in the Ising case and the autocorrelation time reaches a maximal value  $\tau \simeq 7$  at the second peak. Again, the autocorrelation time evolves slowly with the lattice size.

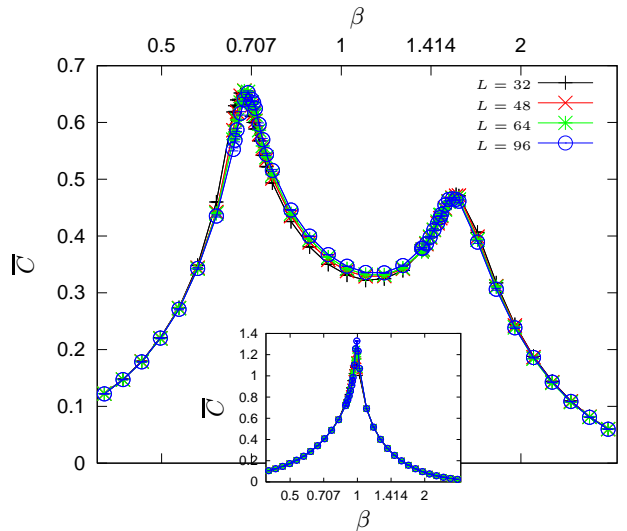


FIG. 5. (Color online) Average specific heat of the Ising model ( $q = 2$ ), with a disorder strength  $r = 3$  and a correlation exponent  $a = 0.4$  ( $y = 0.75$ ), versus the inverse temperature  $\beta = 1/k_B T$ . The different curves correspond to different lattice sizes ( $L = 32, 48, 64$  and  $96$ ). In the inset, the specific heat in the case of uncorrelated disorder is plotted.

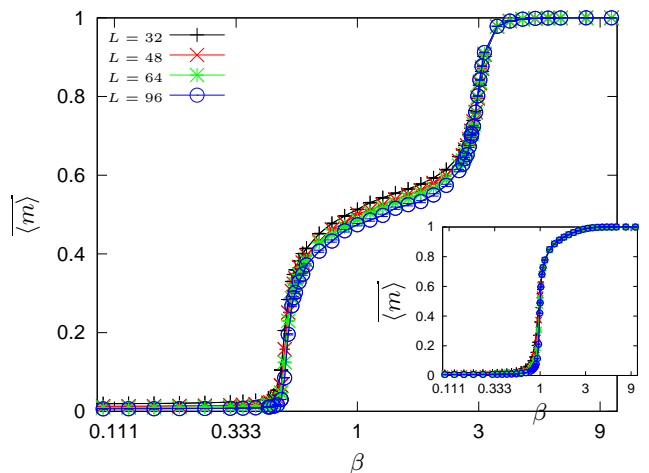


FIG. 6. (Color online) Average magnetization of the 8-state Potts model, with a disorder strength  $r = 7.5$  and a correlation exponent  $a = 0.4$  ( $y = 0.75$ ), versus the inverse temperature  $\beta = 1/k_B T$ . In the inset, magnetization curve in the case of uncorrelated disorder.

#### IV. CRITICAL BEHAVIOR IN THE GRIFFITHS PHASE

In Ref. [29], the critical exponents have been estimated at the self-dual point  $\beta_c = 1$  of the 8-state Potts model with correlated disorder. In the following, the study is extended to the  $q = 2, 4$  and 16-state Potts models, and to several other temperatures in the Griffiths phase. Numerical evidence of the stability of the critical exponents against a variation of the strength of disorder is provided.



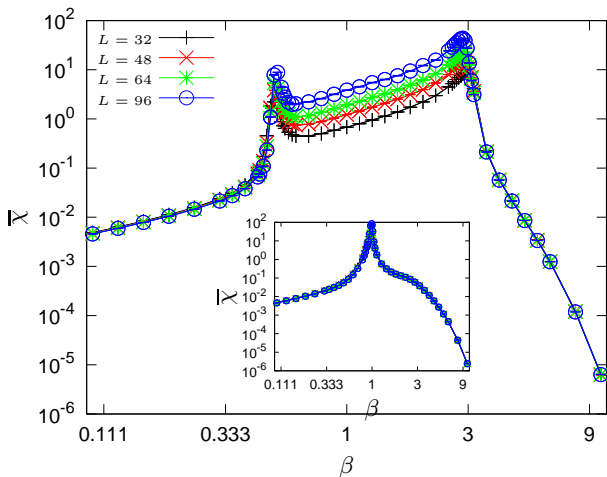


FIG. 7. (Color online) Average susceptibility of the 8-state Potts model, with a disorder strength  $r = 7.5$  and a correlation exponent  $a = 0.4$  ( $y = 0.75$ ), versus the inverse temperature  $\beta = 1/k_B T$ . In the inset, susceptibility in the case of uncorrelated disorder.

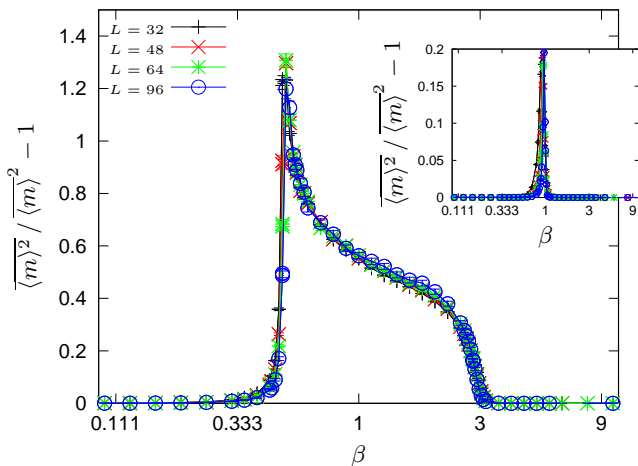


FIG. 8. (Color online) Self-averaging ratio  $R_m$  of magnetization of the 8-state Potts model, with a disorder strength  $r = 7.5$  and a correlation exponent  $a = 0.4$  ( $y = 0.75$ ), versus the inverse temperature  $\beta = 1/k_B T$ . In the inset, ratio in the case of uncorrelated disorder.

Monte Carlo simulations were performed for lattice sizes  $L = 16, 24, 32, 48, 64, 96, 128, 192$ , and  $256$ . The thermodynamic quantities were averaged over a number of disorder configurations proportional to  $1/L^2$ . For the largest lattice size ( $L = 256$ ), 10240 disorder configurations were generated while for  $L = 64$  for example, this number is raised up to 163840. For each disorder configuration, 5000 Monte Carlo steps are performed. The critical exponents  $\beta/\nu$ ,  $\gamma/\nu$  and  $\nu$  are determined by Finite-Size Scaling of the average quantities:

$$\langle m^n \rangle^{1/n} \sim L^{-\beta/\nu},$$

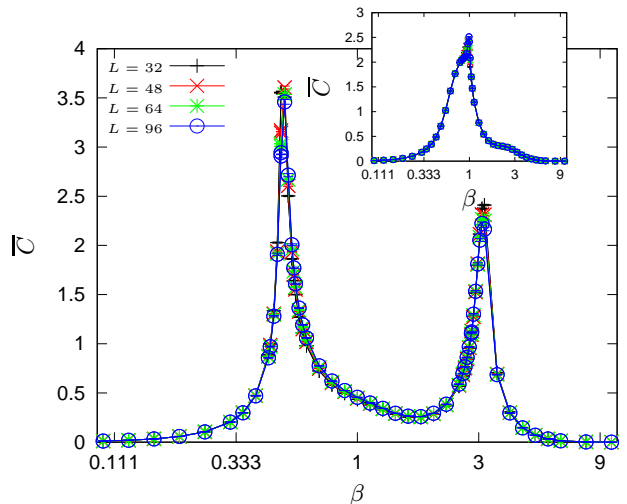


FIG. 9. (Color online) Average specific heat of the 8-state Potts model, with a disorder strength  $r = 7.5$  and a correlation exponent  $a = 0.4$  ( $y = 0.75$ ), versus the inverse temperature  $\beta = 1/k_B T$ . In the inset, the specific heat in the case of uncorrelated disorder.

$$\begin{aligned} \bar{\chi} &= \beta L^d [\langle m^2 \rangle - \langle m \rangle^2] \sim L^{\gamma/\nu}, \\ -\frac{d \ln \langle m \rangle}{d\beta} &= L^d \frac{\langle m e \rangle - \langle m \rangle \langle e \rangle}{\langle m \rangle} \sim L^{1/\nu} \end{aligned} \quad (20)$$

where the moments of order  $n = 1, 2, 3$  and  $4$  of the magnetization are considered. To take into account the possibility of scaling corrections, relatively strong for the average susceptibility, power-law fits are successively performed in the windows  $[L_{\min}, 256]$  where the smallest lattice size  $L_{\min}$  is iteratively increased. The different fits lead to  $L_{\min}$ -dependent effective critical exponents. Because of scaling corrections, these exponents do not reach a plateau at large  $L_{\min}$ , but rather vary continuously with  $L_{\min}$ . An extrapolation of these effective exponents in the limit  $1/L_{\min} \rightarrow 0$  is performed. For most of the observables, it is sufficient to consider an extrapolation with a polynomial of degree 1 in  $1/L_{\min}$ .

Note that the critical exponents  $\beta/\nu$ ,  $\gamma/\nu$  and  $\nu$  were defined only through Finite-Size Scaling of thermodynamic quantities. It is not clear whether a scaling law with a reduced temperature exists or not in the thermodynamic limit. The average magnetic susceptibility  $\bar{\chi}$  for example diverges at all temperatures in the Griffiths phase. It is therefore difficult to imagine how a scaling law such as  $|T - T_c|^\gamma$  could be defined for a temperature  $T$  inside the Griffiths phase.

Among the various moments of magnetization that were considered, the second one displays the smallest scaling corrections. As can be seen on Fig. 10 in the case of the Ising model, the effective exponent  $\beta/\nu$  does not vary much with the lowest lattice size  $L_{\min}$  entering into the power-law fit of  $\langle m^2 \rangle^{1/2}$ . For the average magnetization and the moments of order 3 and

TABLE I. Critical exponent  $\beta/\nu$  extrapolated from the Finite-Size Scaling of the second moment  $\overline{\langle m^2 \rangle}^{1/2}$  of magnetization at the self-dual point  $\beta_c = 1$ . The estimates for uncorrelated disorder can be compared with the exact value  $1/8$  ( $q = 2$ ) and the transfer matrix estimates  $0.1419(1)$  ( $q = 4$ ),  $0.1514(2)$  ( $q = 8$ ) from Ref. [42].

$y$	0	0.25	0.5	0.75	1	1.25	Uncorr. Dis.
$q = 2, r = 2$	0.046(6)	0.051(7)	0.059(6)	0.069(6)	0.078(5)	0.102(7)	0.1250(7)
$q = 2, r = 3$	0.049(7)	0.050(5)	0.060(4)	0.073(5)	0.082(6)	0.102(4)	0.1238(11)
$q = 4, r = 4$	0.052(6)	0.049(7)	0.064(6)	0.071(6)	0.088(7)	0.102(5)	0.139(2)
$q = 8, r = 6$	0.053(6)	0.057(7)	0.066(7)	0.075(6)	0.092(6)	0.104(5)	0.150(2)
$q = 8, r = 7.5$	0.052(6)	0.059(5)	0.067(6)	0.076(6)	0.087(5)	0.104(4)	0.150(2)
$q = 8, r = 9$	0.052(5)	0.056(7)	0.068(7)	0.074(6)	0.088(5)	0.108(8)	0.149(3)
$q = 16, r = 10$	0.052(5)	0.056(6)	0.066(7)	0.072(7)	0.089(5)	0.108(5)	0.159(3)

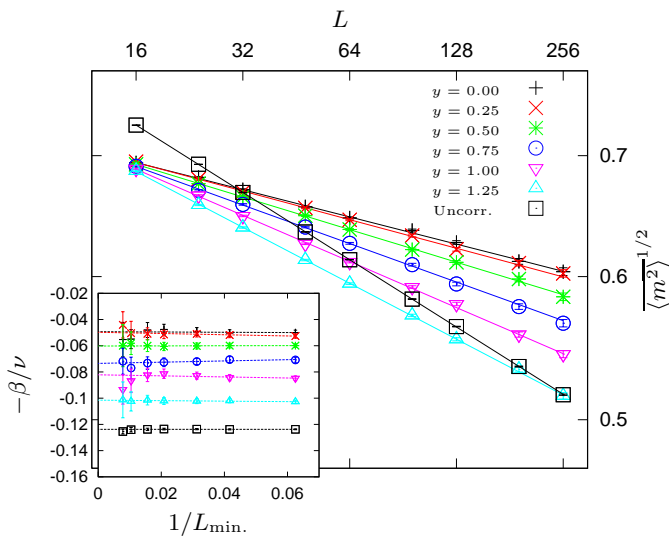


FIG. 10. (Color online) Finite-Size Scaling of the second moment  $\overline{\langle m^2 \rangle}^{1/2}$  of the magnetization of the Ising model ( $q = 2$ ) with a disorder strength  $r = 3$  at the self-dual point  $\beta_c = 1$ . The different curves correspond to different disorder correlation exponents, referred to by the parameter  $y$  of the auxiliary Ashkin-Teller model. The curve with the legend Uncorr. corresponds to the Ising model with uncorrelated disorder. In the inset, effective exponents obtained by fitting the data in the window  $[L_{\min}; 256]$  versus  $1/L_{\min}$ . The straight line is a linear fit of these exponents.

4, a slow linear variation of these exponents is observed. A linear extrapolation leads in the limit  $L_{\min} \rightarrow 0$  to exponents compatible with those obtained from the second moment. The different exponents at the self-dual point  $\beta_c = 1$  are collected in Table I. The exponents do not show any significant dependence on the strength of disorder  $r$ . As already observed in the case of uncorrelated disorder, the amplitude of the scaling corrections depends on  $r$ . More interesting is the fact that the exponents  $\beta/\nu$  do not depend on the number of states  $q$  of the Potts model. As mentioned in the introduction, such a behavior is also observed in the generalization of the McCoy-Wu model to Potts spins. However, the

estimates of  $\beta/\nu$  are remarkably different from the exact value  $\beta/\nu = (3 - \sqrt{5})/4$  at the McCoy-Wu-Fisher fixed point. Furthermore, it can be observed in Table I that the exponent  $\beta/\nu$  increases when the disorder correlations decay faster, i.e. when  $y$ , and therefore  $a$ , increases.  $\beta/\nu$  remains always smaller than in the case of uncorrelated disorder. Such a behavior was also observed for the McCoy-Wu model with correlated disorder in the longitudinal direction [21]. However, the magnetic scaling dimension was shown to be  $\beta/\nu \simeq a/2$  in this model while this exponent is closer to  $a/5$  in the Potts model with correlated disorder. The dependence of  $\beta/\nu$  on  $a$  also contradicts Weinrib and Halperin calculation for which  $\beta/\nu = \mathcal{O}(\epsilon^2)$  in 2D. Therefore, the Potts model with the correlated disorder considered in this paper belongs to a distinct universality class.

The independence of the exponents with the number of states  $q$  contrasts with the case of the Potts model with uncorrelated disorder for which an increase of  $\beta/\nu$  with  $q$  was shown. A very small dependence of  $\beta/\nu$  on  $q$ , compatible with error bars, cannot be completely excluded. Note that in the case of the McCoy-Wu model with correlated disorder, the exponent  $\beta/\nu$  is a continuous function of the correlation exponent  $a$ , even at  $a = 1$  corresponding in this case to uncorrelated disorder [21]. If the same occurs for the isotropic Potts model with correlated disorder, then one should expect a dependence on  $q$  for exponents  $a < 2$  because such a dependence exists for uncorrelated disorder, i.e. for  $a \geq 2$ . This hypothesis could be tested with values of  $a$  close to 2. Unfortunately, the use of the Ashkin-Teller as an auxiliary model to generate the disorder configurations does not allow to go beyond  $a = 3/4$  ( $y = 4/3$ ) and therefore closer to the point  $a = 2$ . Another possible scenario is that the RG flow for the Potts model with correlated disorder is similar to the case studied by Weinrib and Halperin. For small values  $a < d = 2$ , the independence of the exponent  $\beta/\nu$  on  $q$  could be explained by a critical behavior which is controlled by the same correlated-disorder fixed point for all Potts models. Above  $a = d = 2$ , the latter becomes unstable and the critical behavior is then

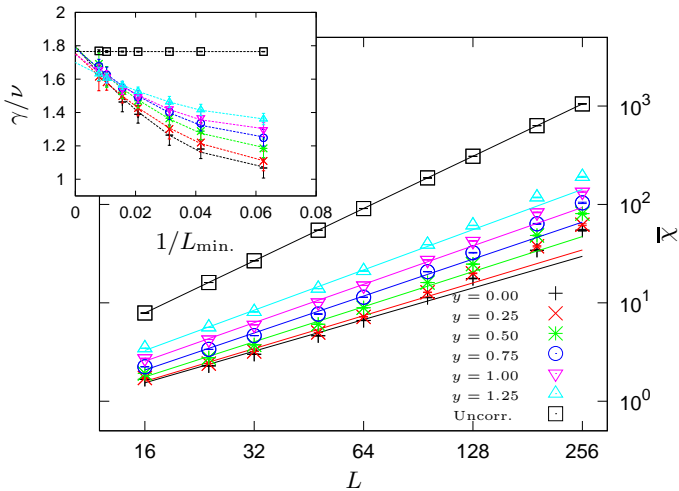


FIG. 11. (Color online) Finite-Size Scaling of the average susceptibility  $\bar{\chi}$  of the Ising model ( $q = 2$ ) with a disorder strength  $r = 3$  at the critical point  $\beta_c = 1$ . The different curves correspond to different disorder correlation exponents, referred to by the parameter  $y$  of the auxiliary Ashkin-Teller model. The curve with the legend Unccorr. corresponds to the Ising model with uncorrelated disorder. In the inset, effective exponents obtained by fitting the data in the window  $[L_{\min}; 256]$  versus  $1/L_{\min.}$ . The solid line is a parabolic fit of these exponents.

governed by the short-range or uncorrelated fixed point where the exponents are known to be  $q$ -dependent.

In the Griffiths phase, the dependence of the exponents on the temperature was tested for the Ising and 8-state Potts models. Estimates of  $\beta/\nu$  are given in Table II. In the Ising case, only one temperature was tested and the corresponding estimates of the exponent  $\beta/\nu$  are incompatible with the value measured at the self-dual point for all parameters  $y \geq 0.5$ . In the Potts case, the Griffiths phase is larger and three well separated temperatures were considered. The exponent  $\beta/\nu$  clearly increases with the temperature for all values of  $y$ . The Griffiths phase is therefore not described by a unique fixed point. This result corroborates the existence of a non-constant asymptotic value of  $R_m$ , supposed to be universal, in the Griffiths phase.

The estimation of the exponent  $\gamma/\nu$  from the Finite-Size Scaling of the magnetic susceptibility is much more difficult. Much stronger scaling corrections are present, especially for small values of  $y$ . These corrections manifest themselves on Fig. 11 as a gap between the numerical data at large lattice sizes and the power-law fit plotted as a continuous line. The effective exponents indeed start with values in the range  $[1.1; 1.3]$  and then increase as more and more small lattice sizes are removed from the fit (see inset of Fig. 11). When only lattice sizes  $L \geq 128$  are taken into account in the fit, the effective exponents take values around 1.6 – 1.7, the value reported in Ref. [29]. On the figure, the effective exponents increase with the parameter  $y$  and tend towards a value close to the ex-

ponent of the uncorrelated disorder. Because of the curvature displayed by the effective exponents when plotted versus  $1/L_{\min.}$ , a simple linear extrapolation, like in the case of magnetization, does not take into account reliably the scaling corrections. It turns out that the exponents fall nicely on the parabolic fit represented on the figure. However, the use of a polynomial of degree 2 reduces the number of degrees of freedom of the fit, and thus increases the error bar and lowers the stability of the extrapolated exponents. The latter are given in Tables III and IV. No significant dependence on the number of states  $q$ , the strength of disorder  $r$ , nor the temperature in the Griffiths phase can be noticed. While the estimates of  $\gamma/\nu$  are compatible between each other, half of them are not compatible with the hyperscaling relation

$$\frac{\gamma}{\nu} = d - 2\frac{\beta}{\nu}. \quad (21)$$

On Fig. 12, the ratio  $\bar{\chi} / L^d \langle m \rangle^2$  is plotted versus the lattice size in the case of the Ising model. This quantity is expected to scale as  $L^0$  when the hyperscaling relation Eq. 21 holds. A power-law behavior is indeed observed at large lattice sizes, though with a smaller exponent than at small lattice sizes. A fit over the three largest lattice sizes leads to negative exponents, compatible within error bars with zero, i.e. the hyperscaling relation, in only 20% of all cases considered. This statement is also true at different temperatures in the Griffiths phase. Of course, we cannot completely exclude the possibility of a restoration of the hyperscaling relation at larger lattice sizes. In the case of uncorrelated disorder, the data are in much better agreement with the hyperscaling relation.

As commented in the first section, the specific heat does not seem to display any divergence in the Griffiths phase. Even with larger lattice sizes, up to  $L = 256$ , it is not possible to isolate any singular part from a regular background. It means that the specific heat exponent  $\alpha/\nu$  is therefore smaller or equal to zero.

The Finite-Size Scaling of the derivative of the logarithm of the average magnetization with respect to temperature gives access to the exponent  $\nu$  [43]. In contrast to the magnetic susceptibility, a linear fit of the  $L_{\min.}$ -dependent effective exponents is sufficient to properly take into account the scaling corrections (see Fig. 13). The extrapolated exponents are given in Tables V and VI. They turn out to be much larger than in the case of uncorrelated disorder for which  $\nu \simeq 1$  [44]. In a few cases, the extrapolation procedure appears to be unstable: several spurious values can be seen in the tables (for example for  $q = 8, r = 7.5, y = 0$  or  $q = 2, \beta = 1.2$ ). From the rest of the data, the same trends as for magnetization are observed: the exponents do not significantly vary with the strength of disorder  $r$ , nor the number of states  $q$ . However, in contrast to magnetization, no significant dependence on temperature can be seen, apart for  $y = 1.25$ . More accurate values would be necessary. Note that the exponent  $\nu$  takes values incompatible with the Weinrib-Halperin prediction  $\nu = 2/a$  for the  $O(n)$

TABLE II. Critical exponent  $\beta/\nu$  extrapolated from the Finite-Size Scaling of the second moment  $\overline{\langle m^2 \rangle}^{1/2}$  of magnetization at different temperatures in the Griffiths phase.

$y$	0	0.25	0.5	0.75	1	1.25
$q = 2, \beta = 1$	0.049(7)	0.050(5)	0.060(4)	0.073(5)	0.082(6)	0.102(4)
$q = 2, \beta = 1.2$	0.040(6)	0.044(5)	0.048(4)	0.050(4)	0.063(4)	0.043(7)
$q = 8, \beta = 0.75$	0.057(7)	0.062(5)	0.073(5)	0.092(6)	0.110(7)	0.138(6)
$q = 8, \beta = 1$	0.052(6)	0.059(5)	0.067(6)	0.076(6)	0.087(5)	0.104(4)
$q = 8, \beta = 1.5$	0.050(5)	0.052(5)	0.055(5)	0.64(7)	0.073(7)	0.082(5)
$q = 8, \beta = 2$	0.041(6)	0.045(5)	0.052(6)	0.056(6)	0.061(4)	0.052(4)

TABLE III. (Color online) Critical exponent  $\gamma/\nu$  extrapolated from the Finite-Size Scaling of the average susceptibility  $\overline{\chi}$  at the self-dual point  $\beta_c = 1$ . A polynomial of degree 2 was used for the extrapolation. The estimates for uncorrelated disorder can be compared with the exact value  $7/4$  ( $q = 2$ ) and the transfer matrix estimates  $1.7162(2)$  ( $q = 4$ ),  $1.6972(4)$  ( $q = 8$ ) from Ref. [42] assuming that hyperscaling holds.

$y$	0	0.25	0.5	0.75	1	1.25	Uncorr. Dis.
$q = 2, r = 2$	1.66(7)	1.73(9)	1.69(12)	1.66(7)	1.64(6)	1.64(7)	1.759(6)
$q = 2, r = 3$	1.80(7)	1.76(8)	1.79(10)	1.78(7)	1.75(6)	1.70(4)	1.766(8)
$q = 4, r = 4$	1.84(9)	1.80(7)	1.80(5)	1.74(5)	1.81(5)	1.77(7)	1.717(13)
$q = 8, r = 6$	1.77(12)	1.77(7)	1.79(7)	1.80(8)	1.77(6)	1.75(7)	1.68(2)
$q = 8, r = 7.5$	1.77(7)	1.75(8)	1.78(6)	1.78(8)	1.75(7)	1.74(5)	1.70(3)
$q = 8, r = 9$	1.78(9)	1.84(11)	1.80(8)	1.77(6)	1.72(6)	1.74(6)	1.71(2)
$q = 16, r = 10$	1.78(10)	1.80(12)	1.79(9)	1.78(10)	1.72(6)	1.74(5)	1.75(3)

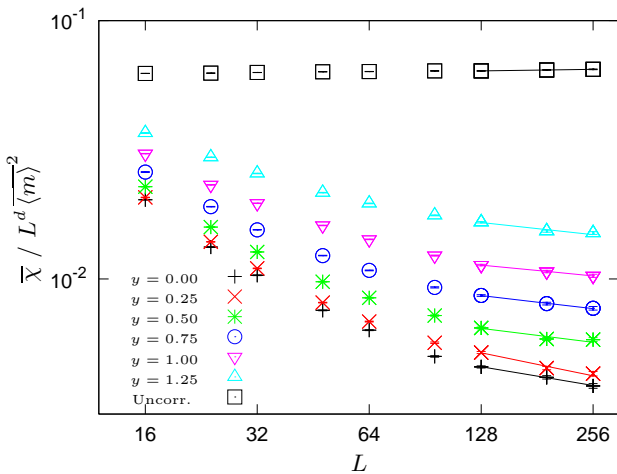


FIG. 12. (Color online)  $\overline{\chi} / L^d \overline{\langle m^2 \rangle}^2$  versus the lattice size  $L$  for the Ising model ( $q = 2$ ) with a disorder strength  $r = 3$  at the self-dual point  $\beta_c = 1$ . According to the hyperscaling relation, this ratio should scale as  $L^0$ . The straight line is a power-law fit over the three last lattice sizes. The slopes, as given by the fit, are  $-0.24(5)$ ,  $-0.38(10)$ ,  $-0.3(2)$ ,  $-0.30(5)$ ,  $-0.31(6)$ ,  $-0.18(3)$  for  $y = 0.00, 0.25, 0.50, 0.75, 1.00$  and  $1.25$ . For uncorrelated disorder, this value is  $0.012(10)$ .

model with (Gaussian) correlated disorder. For comparison, the latter would give  $1/\nu = 0.125, 0.143, 0.167, 0.2, 0.25$  and  $0.333$  for the values of  $a$  that were considered.

Finally, note that the hyperscaling relation  $\frac{\alpha}{\nu} = \frac{2}{\nu} - d$  leads, with the estimates of  $\nu$  reported in Tables V and VI, to negative specific heat exponents  $\frac{\alpha}{\nu} < -1.7$ . Because of the regular contribution to the specific heat, this prediction cannot be tested.

## V. DISORDER FLUCTUATIONS AND HYPERSCALING VIOLATION

As pointed out in the previous section, the average susceptibility diverges with an exponent  $\gamma/\nu$  which is close, but not perfectly compatible, with the hyperscaling relation and the magnetization exponent  $\beta/\nu$ . As pointed out in Ref [29], this violation of hyperscaling is the result of large disorder fluctuations, as in the 3D random-field Ising model [45] (RFIM). We briefly describe in the following the arguments of [29]. The average magnetic susceptibility, as given by the derivative of the average magnetization with respect to an external magnetic field, can be decomposed as

$$\begin{aligned} \overline{\chi} &= \beta L^d [\overline{\langle m^2 \rangle} - \overline{\langle m \rangle}^2] \\ &= \underbrace{\beta L^d [\overline{\langle m^2 \rangle} - \overline{\langle m \rangle}^2]}_{=\chi_1} - \underbrace{\beta L^d [\overline{\langle m \rangle}^2 - \overline{\langle m \rangle}^2]}_{=\chi_2} \quad (22) \end{aligned}$$

The two terms, denoted  $\chi_1$  and  $\chi_2$ , scale differently from the average susceptibility, i.e. their difference. The second term  $\chi_2$  is the numerator of the ratio  $R_m$ , defined

TABLE IV. Critical exponent  $\gamma/\nu$  extrapolated from the Finite-Size Scaling of the average susceptibility  $\overline{\chi}$  at different temperatures in the Griffiths phase. A polynomial of degree 2 was used for the extrapolation.

$y$	0	0.25	0.5	0.75	1	1.25
$q = 2, \beta = 1$	1.80(7)	1.76(8)	1.79(10)	1.78(7)	1.75(6)	1.70(4)
$q = 2, \beta = 1.2$	1.64(5)	1.70(8)	1.73(8)	1.71(5)	1.76(4)	1.69(4)
$q = 8, \beta = 0.75$	1.80(11)	1.86(8)	1.78(9)	1.68(6)	1.71(7)	1.68(4)
$q = 8, \beta = 1$	1.77(7)	1.75(8)	1.78(6)	1.78(8)	1.75(7)	1.74(5)
$q = 8, \beta = 1.5$	1.80(10)	1.70(8)	1.72(6)	1.77(6)	1.78(8)	1.78(5)
$q = 8, \beta = 2$	1.68(8)	1.74(9)	1.78(8)	1.74(6)	1.71(8)	1.78(4)

TABLE V. Critical exponent  $1/\nu$  extrapolated from the Finite-Size Scaling of the quantity  $-\frac{d}{d\beta} \ln \overline{\langle m \rangle}$  at the self-dual point  $\beta_c = 1$ . For uncorrelated disorder, estimates of  $\nu$  slightly above 1, but usually compatible, were reported in the literature [2, 10]. In the case  $q = 2, \nu = 1$  (with logarithmic corrections) since uncorrelated disorder is marginally irrelevant.

$y$	0	0.25	0.5	0.75	1	1.25	Uncorr. Dis.
$q = 2, r = 2$	0.041(10)	0.065(12)	0.099(13)	0.116(13)	0.11(2)	0.14(2)	0.969(4)
$q = 2, r = 3$	0.028(13)	0.044(11)	0.086(10)	0.112(9)	0.11(2)	0.13(2)	0.944(5)
$q = 4, r = 4$	0.033(12)	0.041(13)	0.082(12)	0.103(14)	0.113(14)	0.116(13)	0.985(7)
$q = 8, r = 6$	0.026(11)	0.05(2)	0.08(2)	0.101(11)	0.115(11)	0.113(11)	0.965(11)
$q = 8, r = 7.5$	0.25(10)	0.047(12)	0.083(9)	0.107(10)	0.111(9)	0.114(7)	0.976(9)
$q = 8, r = 9$	0.018(11)	0.041(12)	0.075(12)	0.097(11)	0.102(9)	0.109(12)	0.972(7)
$q = 16, r = 10$	0.022(10)	0.04(2)	0.069(10)	0.083(14)	0.101(10)	0.113(9)	1.02(3)

by Eq. 18. Because the latter tends to a finite constant in the Griffiths phase (see Fig. 18),  $\overline{\langle m \rangle^2} - \langle m \rangle^2$  scales as  $\langle m \rangle^2$ , i.e. as  $L^{-2\beta/\nu}$ . Therefore, including the  $L^d$  prefactor, the susceptibility  $\chi_2$  scales as  $L^{d-2\beta/\nu}$ , i.e. precisely as predicted by the hyperscaling relation Eq. 21. The numerical study of the Finite-Size Scaling of  $\chi_1$  reveals that it displays the same scaling behavior. As can be seen on Fig. 14 in the case of the Ising model and Fig. 15 for the 8-state Potts model,  $\chi_1$  is very different from the average susceptibility. Instead of two peaks separating a region of divergent susceptibility, a single broader peak is observed. Uncorrelated disorder leads to a thinner and thinner peak, like the average susceptibility. For all temperatures in the Griffiths phase,  $\chi_1$  diverges algebraically with an exponent that will be denoted  $(\gamma/\nu)^*$  in the following [47]. The exponent  $(\gamma/\nu)^*$  is estimated by following the same procedure as in the previous section. Effective exponents are first extracted by varying the fitting window. In contrast to the average magnetic susceptibility,  $\chi_1$  displays relatively weak scaling corrections so the effective exponents can safely be extrapolated with a linear fit. The extrapolated exponents  $(\gamma/\nu)^*$  are presented in Tables VII and VIII.  $(\gamma/\nu)^*$  depends on the disorder correlation exponent  $a$  but not on the number of states  $q$ , nor the strength of disorder  $r$ . The temperature dependence in the Griffiths phase is clearly seen for the largest values of  $y$ . As claimed above, the exponents are compatible with the hyperscaling relation and the estimates of  $\beta/\nu$  for any Potts model and at any temperature in

the Griffiths phase.

Not only  $\chi_1$  and  $\chi_2$  have the same scaling behavior but their dominant scaling terms also have the same amplitude  $A$ , i.e.

$$\chi_i = AL^{d-2\beta/\nu}(1 + B_i L^{-\omega_i} + \dots), \quad (i = 1, 2). \quad (23)$$

As a consequence, their difference behaves at large lattice sizes as

$$\overline{\chi} = \chi_1 - \chi_2 \sim AB_1 L^{d-2\beta/\nu-\omega_1} - AB_2 L^{d-2\beta/\nu-\omega_2} \quad (24)$$

i.e. with a scaling dimension  $\gamma/\nu = d - 2\beta/\nu - \min(\omega_1, \omega_2)$ . Our estimates of  $\gamma/\nu$ , as given in Tables III and IV, and the analysis of the ratio  $\overline{\chi}/L^d \overline{\langle m \rangle^2}$  (see for example Fig. 12) indicate that the deviation from the hyperscaling relation, i.e.  $\min(\omega_1, \omega_2)$ , is small (of order 0.1–0.3). The only possibility for a restoration of hyperscaling at large lattice sizes is that the largest correction of either  $\chi_1$  or  $\chi_2$  diverge logarithmically, i.e.  $\omega_1 = 0$  or  $\omega_2 = 0$ . In any other cases, one should expect a violation of hyperscaling. Note that the average susceptibility  $\overline{\chi}$  is two to three orders of magnitude smaller than both  $\chi_1$  and  $\chi_2$ , which means that  $B_i \simeq 10^{-2}$ . This is in agreement with the observation that  $\chi_1$  and  $\chi_2$  only display weak scaling corrections. To check that both  $\chi_1$  and  $\chi_2$  have the same dominant amplitude  $A$ , their ratio was analyzed. Two particular cases are presented on Fig. 16. On the left, the ratio  $\chi_1/\chi_2$  for the Ising model goes to the expected limit 1 for all parameters  $y$  considered while for uncorrelated disorder, a very different

TABLE VI. Critical exponent  $1/\nu$  estimated from the Finite-Size Scaling of the quantity  $-\frac{d}{d\beta} \ln \overline{\langle m \rangle}$  at different temperatures in the Griffiths phase.

$y$	0	0.25	0.5	0.75	1	1.25
$q = 2, \beta = 1$	0.028(13)	0.044(11)	0.086(10)	0.112(9)	0.11(2)	0.13(2)
$q = 2, \beta = 1.2$	-0.03(2)	0.00(2)	0.05(2)	0.059(12)	0.13(2)	0.31(2)
$q = 8, \beta = 0.75$	0.04(2)	0.06(2)	0.09(2)	0.11(2)	0.13(2)	0.187(11)
$q = 8, \beta = 1$	0.025(10)	0.047(12)	0.083(9)	0.107(10)	0.111(9)	0.114(7)
$q = 8, \beta = 1.5$	0.03(2)	0.04(2)	0.07(2)	0.103(14)	0.10(2)	0.146(13)
$q = 8, \beta = 2$	0.01(2)	0.03(2)	0.08(2)	0.079(13)	0.11(2)	0.336(13)

TABLE VII. Critical exponent  $(\gamma/\nu)^*$  extrapolated from the Finite-Size Scaling of the quantity  $\chi_1$  at the self-dual point  $\beta_c = 1$ .

$y$	0	0.25	0.5	0.75	1	1.25	Uncorr. Dis.
$q = 2, r = 2$	1.92(4)	1.91(4)	1.90(4)	1.88(4)	1.86(4)	1.83(4)	1.751(13)
$q = 2, r = 3$	1.91(3)	1.91(3)	1.89(3)	1.87(3)	1.85(3)	1.81(4)	1.75(2)
$q = 4, r = 4$	1.90(3)	1.89(3)	1.88(3)	1.86(3)	1.83(3)	1.79(3)	1.73(2)
$q = 8, r = 6$	1.90(2)	1.89(2)	1.87(2)	1.86(2)	1.82(3)	1.78(2)	1.72(4)
$q = 8, r = 7.5$	1.90(2)	1.90(2)	1.88(2)	1.85(2)	1.82(3)	1.79(3)	1.73(4)
$q = 8, r = 9$	1.91(2)	1.89(2)	1.88(2)	1.85(2)	1.83(3)	1.79(3)	1.75(4)
$q = 16, r = 10$	1.90(2)	1.89(2)	1.88(2)	1.86(2)	1.83(2)	1.78(3)	1.74(4)

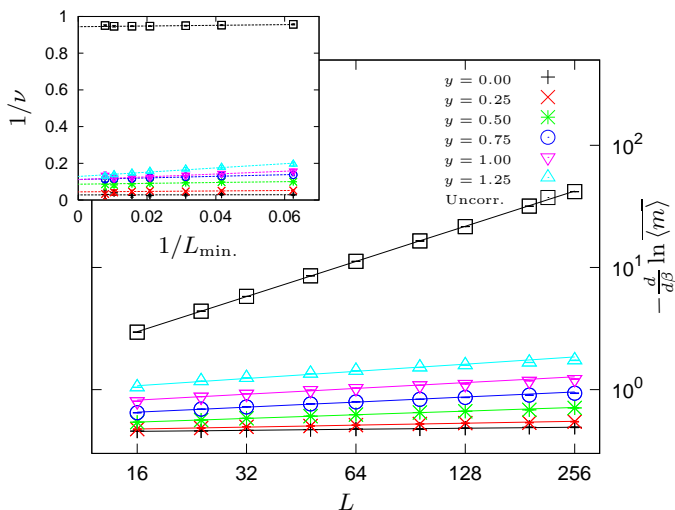


FIG. 13. (Color online) Finite-Size Scaling of  $-\frac{d}{d\beta} \ln \overline{\langle m \rangle}$  for the Ising model ( $q = 2$ ) with a disorder strength  $r = 3$  at the critical point  $\beta_c = 1$ . The different curves correspond to different disorder correlation exponents, referred to by the parameter  $y$  of the auxiliary Ashkin-Teller model. The curve with the legend Uncorr. corresponds to the Ising model with uncorrelated disorder. In the inset, effective exponents  $1/\nu$  obtained by fitting the data in the window  $[L_{\min}; 256]$  versus  $1/L_{\min}$ . The straight line is a linear fit of these exponents.

limit is observed. On the right, this ratio is plotted in the case of the 8-state Potts at several temperatures in the Griffiths phase. Again, the data goes to the limit 1.

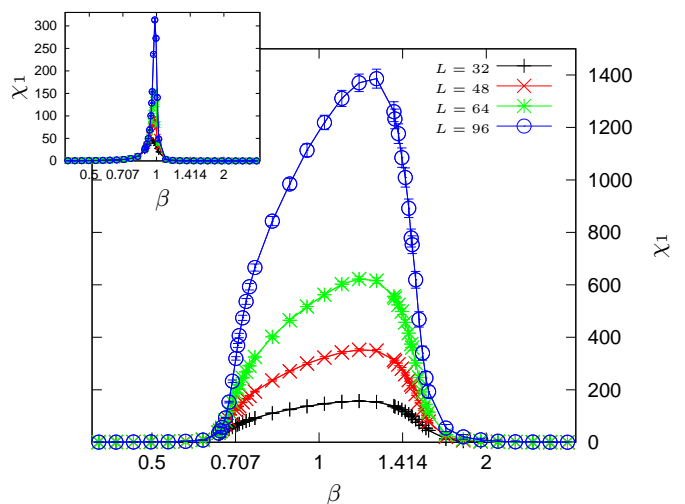


FIG. 14. (Color online) Disorder fluctuations of magnetization  $\chi_1$  of the Ising model ( $q = 2$ ), with a disorder strength  $r = 3$  and a correlation exponent  $a = 0.4$  ( $y = 0.75$ ), versus the inverse temperature  $\beta = 1/k_B T$ . In the inset, disorder fluctuations in the case of uncorrelated disorder.

The same analysis, reproduced for all numbers of states  $q$ , strength of disorder  $r$ , or temperatures in the Griffiths phase, leads to the same conclusion. In all cases, the leading amplitudes of  $\chi_1$  and  $\chi_2$  are shown to be identical. Consequently, the dominant contributions of  $\chi_1$  and  $\chi_2$  cancel out and the hyperscaling relation is broken in the entire Griffiths phase. In the case of uncorrelated disorder, the ratio goes to a value very different from 1

TABLE VIII. Critical exponent  $(\gamma/\nu)^*$  extrapolated from the Finite-Size Scaling of the quantity  $\chi_1$  at different temperatures in the Griffiths phase.

$y$	0	0.25	0.5	0.75	1	1.25
$q = 2, \beta = 1$	1.91(3)	1.91(3)	1.89(3)	1.87(3)	1.85(3)	1.81(4)
$q = 2, \beta = 1.2$	1.96(3)	1.95(4)	1.93(4)	1.92(4)	1.92(4)	1.79(6)
$q = 8, \beta = 0.75$	1.88(2)	1.87(2)	1.85(2)	1.82(2)	1.77(2)	1.72(2)
$q = 8, \beta = 1$	1.90(2)	1.90(2)	1.88(2)	1.85(2)	1.82(3)	1.79(3)
$q = 8, \beta = 1.5$	1.92(3)	1.92(3)	1.90(2)	1.89(2)	1.87(3)	1.84(3)
$q = 8, \beta = 2$	1.94(3)	1.94(3)	1.92(3)	1.91(3)	1.90(3)	1.78(5)

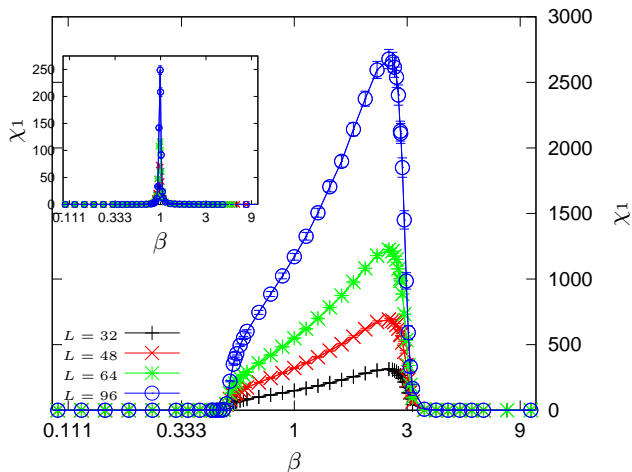


FIG. 15. (Color online) Disorder fluctuations of magnetization  $\chi_1$  of the 8-state Potts model, with a disorder strength  $r = 7.5$  and a correlation exponent  $a = 0.4$  ( $y = 0.75$ ), versus the inverse temperature  $\beta = 1/k_B T$ . In the inset, disorder fluctuations in the case of uncorrelated disorder.

(see left of Fig. 16). Therefore, the dominant contributions of  $\chi_1$  and  $\chi_2$  do not cancel out in this case and the hyperscaling relation is not broken.

The same analysis can be performed in the energy sector. However, as already mentioned, it is not possible to decide whether the hyperscaling relation  $\frac{\alpha}{\nu} = \frac{2}{\nu} - d$  is broken or not because the specific heat does not diverge and therefore its singular part cannot be separated from the regular background. Nevertheless, one can check that the same mechanism is present, which implies that hyperscaling is broken unless the first correction is only logarithmic. The average specific heat is decomposed as

$$\begin{aligned} \overline{C} &= \beta^2 L^d [\overline{\langle e^2 \rangle} - \overline{\langle e \rangle}^2] \\ &= \underbrace{\beta^2 L^d [\overline{\langle e^2 \rangle} - \overline{\langle e \rangle}^2]}_{=C_1} - \underbrace{\beta^2 L^d [\overline{\langle e \rangle^2} - \overline{\langle e \rangle}^2]}_{=C_2}. \end{aligned} \quad (25)$$

The scaling behavior of  $C_2$  cannot be deduced from the ratio  $R_e$  defined by Eq. 19. In contrast to the magnetic sector,  $R_e$  vanishes in the thermodynamic limit, meaning that the energy density becomes a self-averaging quantity [48]. Both  $C_1$  and  $C_2$  display a behavior with

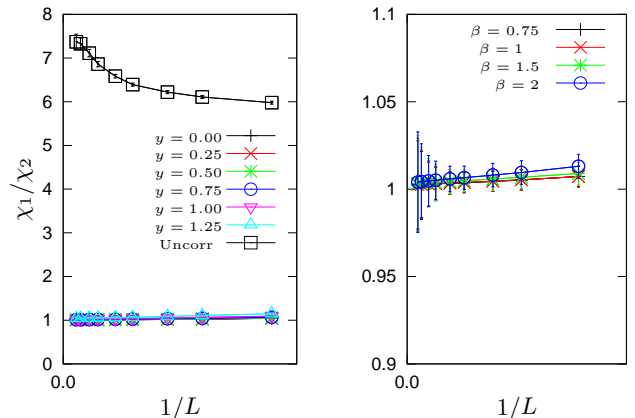


FIG. 16. (Color online) Ratio  $\chi_1/\chi_2$  versus the inverse  $1/L$  of the lattice size for various parameters  $y$  in the case of the Ising model ( $r = 3$ ) on the left and for several temperatures in the Griffiths phase of the 8-state Potts ( $y = 0.75$  and  $r = 7.5$ ) on the right.

temperature very different from the average specific heat. In contrast to  $\overline{C}$ , they diverge in the Griffiths phase and, because of the  $\beta^2$  prefactor, they keep on growing as the temperature is decreased. We have tested the Finite-Size Scaling of  $C_1$  at several temperatures in the Griffiths phase. While the specific heat is almost independent of the lattice size,  $C_1$  diverges algebraically with a large exponent  $(\alpha/\nu)^*$ . As shown in Tables IX and X,  $(\alpha/\nu)^*$  depends only on the disorder correlation exponent  $a$ , and therefore on  $y$ , but not on the number of states  $q$ , the strength of disorder  $r$ , nor the temperature. The estimates are in good agreement with  $d - a$  which means that the energy fluctuations are controlled by the disorder fluctuations. This result implies that a strong coupling  $J_2$  essentially freezes the relative state of the two spins, while a weak one  $J_1$  leads to an irrelevant constraint between them. Amazingly, the ratio  $C_1/C_2$  goes to a constant in excellent agreement with 1 for all temperatures in the Griffiths phase. As a consequence, the dominant contributions of  $C_1$  and  $C_2$  cancel out exactly, leading to an algebraic behavior of the specific heat with a much smaller exponent  $\alpha/\nu \ll (\alpha/\nu)^*$  than both  $C_1$  and  $C_2$ . Since  $\alpha/\nu \leq 0$ , the largest scaling

correction of  $C_1$  and  $C_2$  decays faster than  $L^{-(\alpha/\nu)^*}$ . In the case of uncorrelated disorder, the ratio  $C_1/C_2$  goes to a value different from 1, even though error bars increase rapidly at large lattice sizes and finally include 1. The cancellation does not take place and the equality  $\alpha/\nu = (\alpha/\nu)^*$  is expected.

In the magnetic sector, the exponent  $(\gamma/\nu)^*$  was shown to satisfy the hyperscaling relation  $(\gamma/\nu)^* = d - 2\beta/\nu = d - 2x_\sigma$  with the exponent  $\beta/\nu$ . Assuming that this is also the case in the energy sector,  $(\alpha/\nu)^*$  is conjectured to satisfy the hyperscaling relation  $(\alpha/\nu)^* = d - 2x_\varepsilon$  where  $x_\varepsilon$  is the energy scaling dimension. As discussed above,  $(\alpha/\nu)^*$  is compatible with  $d - a$  which implies  $x_\varepsilon = a/2$ , i.e. the energy-energy correlation functions, decaying as  $r^{-2x_\varepsilon}$ , are determined by the coupling correlations in the Griffiths phase.

The same procedure is applied to the quantity

$$\begin{aligned} -\frac{d}{d\beta} \ln \overline{\langle m \rangle} &= L^d \frac{\overline{\langle me \rangle} - \overline{\langle m \rangle} \overline{\langle e \rangle}}{\overline{\langle m \rangle}} \quad (26) \\ &= \underbrace{L^d \frac{\overline{\langle me \rangle} - \overline{\langle m \rangle} \overline{\langle e \rangle}}{\overline{\langle m \rangle}}}_{=X_1} - \underbrace{L^d \frac{\overline{\langle m \rangle} \overline{\langle e \rangle} - \overline{\langle m \rangle} \overline{\langle e \rangle}}{\overline{\langle m \rangle}}}_{=X_2} \end{aligned}$$

Both terms in the second line diverge algebraically in the Griffiths phase. Like the specific heat, the exponent  $1/\nu^*$  extracted from this divergence does not depend on the number of states  $q$ , the strength of disorder  $r$ , nor the temperature but only on disorder correlations, i.e. on  $y$  or equivalently on  $a$ . As can be observed in Tab. XI and XII, the numerical estimates are compatible with  $1/\nu^* = d - a/2$ . Interestingly, the exponents  $(\alpha/\nu)^*$  and  $1/\nu^*$  are compatible with the hyperscaling relation

$$\left(\frac{\alpha}{\nu}\right)^* = \frac{2}{\nu^*} - d. \quad (27)$$

This relation is of course exactly satisfied by the two conjectures  $(\alpha/\nu)^* = d - a$  et  $1/\nu^* = d - a/2$ . Assuming  $1/\nu^* = d - x_\varepsilon$ , the same value of the energy scaling dimension, i.e.  $x_\varepsilon = a/2$ , is obtained. The ratio  $X_1/X_2$  is compatible with the value 1 at all temperatures in the Griffiths phase. Therefore, the dominant contributions of  $X_1$  and  $X_2$  cancel out, which explains the very different exponent  $1/\nu \ll 1/\nu^*$  with which the difference  $-\frac{d}{d\beta} \ln \overline{\langle m \rangle} = X_1 - X_2$  diverge. We note that the correction exponent  $\omega = 1/\nu^* - 1/\nu$  that is responsible for such a large difference is not an integer, i.e. the largest correction is not analytic, and depends on the disorder correlation exponent  $a$ . It is however smaller than for the specific heat.

## VI. CONCLUSIONS

A Potts model with algebraically-decaying coupling correlations is studied by large-scale Monte Carlo sim-

ulations. Such a disorder is obtained by coupling the polarization density of a quenched self-dual Ashkin-Teller model to the energy density of the Potts model. By construction, the disorder is not generated by a Gaussian action and therefore, multiple-point correlation functions are not trivially given by the Wick theorem. As a consequence, the model is outside of the scope considered by Weinrib and Halperin in the case of the  $O(n)$ -model. Our model shares two important similarities with the McCoy-Wu model: a Griffiths phase occurs in a finite range of temperatures around the self-dual point and scaling dimensions are independent of the number of Potts states  $q$ . This is probably a general feature of random systems with sufficiently strong disorder correlations.

In contrast to energy, magnetization is shown to be non self-averaging in the Griffiths phase. Magnetization and magnetic susceptibility display algebraic behaviors with the lattice size at all temperatures in the phase Griffiths phase. The exponent  $\beta/\nu$  does not depend on the number of Potts states  $q$  nor the strength of disorder  $r$  but varies with the disorder correlation exponent  $a$  and the temperature in the Griffiths phase. Our estimates of  $\gamma/\nu$  display a small violation of the hyperscaling relation. This violation is shown to be caused by the exact cancellation of two terms,  $\chi_1$  and  $\chi_2$ , whose difference gives the average susceptibility, as in the 3D Random-Field Ising model. Such a mechanism leads to an hyperscaling violation unless the largest correction of any of the two terms  $\chi_1$  or  $\chi_2$  diverge only logarithmically. From the scaling of  $\chi_1$  and  $\chi_2$ , an exponent  $(\gamma/\nu)^*$  satisfying the hyperscaling relation can be extracted. Because the specific heat does not diverge, the exponent  $\alpha/\nu$  is negative or zero. However, it can also be written as the difference of two diverging terms. From them, an exponent  $(\alpha/\nu)^*$  is defined and shown to be compatible with  $d - a$  for any number of Potts state and any temperature in the Griffiths phase. Because the same mechanism than in the magnetic sector takes place, the energy scaling dimension is conjectured to be given by  $(\alpha/\nu)^* = d - 2x_\varepsilon$  which implies  $x_\varepsilon = a/2$ . The exponent  $\nu$  is extracted from the Finite-Size Scaling of  $\frac{d}{d\beta} \overline{\langle m \rangle}$  at different temperatures of the Griffiths phase. Again, this quantity can be written as a difference of two terms, diverging with a much larger exponent  $1/\nu^*$  compatible with  $d - a/2$ , again for any number of Potts states and any temperature in the Griffiths phase.

Of course, these results have been obtained for finite-size systems so we cannot exclude completely the possibility that the Griffiths phase disappears at much larger lattice sizes and that the hyperscaling relation is restored. Indeed, one could argue that the existence of this Griffiths phase is related to the large fluctuations of the number of strong and weak couplings from sample to sample. These fluctuations are indeed expected to vanish in the thermodynamic limit as  $L^{-a/2}$  but are still very large for the lattice sizes that were considered, much larger than for uncorrelated disorder. If the Griffiths phase is only due to these fluctuations, its width should also vanish in the thermodynamic limit as  $L^{-a/2}$ . The numerical data



TABLE IX. Critical exponent  $(\alpha/\nu)^*$  estimated from the Finite-Size Scaling of the quantity  $C_1$  at the self-dual point  $\beta_c = 1$ . No extrapolation is needed in this case.

$y$	0	0.25	0.5	0.75	1	1.25	Uncorr. Dis.
$q = 2, r = 2$	1.75(2)	1.73(2)	1.68(2)	1.61(2)	1.51(2)	1.35(3)	0.23(6)
$q = 2, r = 3$	1.748(11)	1.730(12)	1.681(13)	1.608(14)	1.506(15)	1.35(2)	0.18(6)
$q = 4, r = 4$	1.749(9)	1.731(10)	1.682(10)	1.610(11)	1.507(12)	1.34(2)	0.28(5)
$q = 8, r = 6$	1.749(8)	1.729(9)	1.681(9)	1.609(9)	1.506(12)	1.343(14)	0.26(5)
$q = 8, r = 7.5$	1.748(8)	1.730(8)	1.681(9)	1.608(10)	1.505(11)	1.344(14)	0.21(5)
$q = 8, r = 9$	1.747(8)	1.729(8)	1.680(9)	1.607(10)	1.503(11)	1.340(13)	0.18(5)
$q = 16, r = 10$	1.747(8)	1.731(9)	1.681(9)	1.606(9)	1.502(10)	1.341(13)	0.20(5)
$d - a$	1.75	1.714	1.667	1.600	1.500	1.333	0

TABLE X. Critical exponent  $(\alpha/\nu)^*$  estimated from the Finite-Size Scaling of the quantity  $C_1$  at different temperatures in the Griffiths phase. No extrapolation is needed in this case.

$y$	0	0.25	0.5	0.75	1	1.25
$q = 2, \beta = 1$	1.748(11)	1.730(12)	1.681(13)	1.608(14)	1.506(15)	1.35(2)
$q = 2, \beta = 1.2$	1.748(12)	1.730(12)	1.682(13)	1.606(14)	1.51(2)	1.34(2)
$q = 8, \beta = 0.75$	1.749(8)	1.731(8)	1.684(9)	1.609(10)	1.506(10)	1.342(13)
$q = 8, \beta = 1$	1.748(8)	1.730(8)	1.681(9)	1.608(10)	1.505(11)	1.344(14)
$q = 8, \beta = 1.5$	1.747(8)	1.729(9)	1.680(9)	1.605(10)	1.503(11)	1.338(14)
$q = 8, \beta = 2$	1.747(8)	1.730(9)	1.680(10)	1.605(10)	1.503(12)	1.340(14)

seems to indicate that it is not the case: the distance between the two peaks of the average magnetic susceptibility on figure 7 is roughly 2.44 for  $L = 32$  and 2.34 for  $L = 96$ . There is therefore a reduction of the width but much smaller than the expected factor  $(32/96)^{-0.2} \simeq 1.25$  for  $y = 0.75$  ( $a = 0.4$ ). The Griffiths phase does not seem to be a consequence of only the fluctuations of the number of strong and weak couplings. Of course, much larger lattice sizes would help to clarify this point. Another possibility would be to study correlated disorder with a larger exponent  $a$ , which is not possible with the two-dimensional Ashkin-Teller model.

Another interesting point would be to understand precisely why the critical behavior observed in this model does not fall into the same universality as the  $\phi^4$  model

studied by Weinrib and Halperin. Further Renormalization Group studies could probably clarify the role of  $n$ -point disorder correlations functions.

## ACKNOWLEDGMENTS

The author is grateful to Sreedhar Dutta for warm discussions and to the Indian Institute for Science Education and Research (IISER) of Thiruvananthapuram where part of this work was done. The author also thanks Francesco Parisen Toldin for having pointed out the fact that  $R_\chi$  decreases with the lattice size  $L$  as  $1/\ln L$  in the case of the Ising model with uncorrelated disorder.

- 
- [1] A. B. Harris *J. Phys. C: Solid State Phys.* **7** 1671 (1974).  
[2] J.L. Cardy, and J.L. Jacobsen *Phys. Rev. Lett.* **79** 4063 (1997), J.L. Jacobsen, and J.L. Cardy *Nucl. Phys. B* **515** 701 (1998), C. Chatelain, and B. Berche *Nucl. Phys. B* **572** 626 (2000).  
[3] A.W.W. Ludwig *Nucl. Phys. B* **285** 97 (1987), A.W.W. Ludwig, and J.L. Cardy *Nucl. Phys. B* **285** 687 (1987), V.I.S. Dotsenko, M. Picco, and P. Pujol *Phys. Lett. B* **347** 113 (1995), V.I.S. Dotsenko, M. Picco, and P. Pujol *Nucl. Phys. B* **455** 701 (1995).  
[4] V.S. Dotsenko, and V.I.S. Dotsenko *Adv. Phys.* **32** 129 (1983), B.N. Shalaev *Sov. Phys. Solid State* **26** 1811 (1984), B.N. Shalaev *Phys. Rep.* **237** 129 (1994), A.W.W. Ludwig *Phys. Rev. Lett.* **61** 2388 (1988), R. Shankar *Phys. Rev. Lett.* **61** 2390 (1988).  
[5] A. Pelissetto, and E. Vicari *Phys. Rev. B* **62** 6393 (2000), P. Calabrese, V. Martín-Mayor, A. Pelissetto, and E. Vicari *Phys. Rev. E* **68** 036136 (2003), H.G. Ballesteros, L.A. Fernández, V. Martín-Mayor, A. Muñoz Sudupe, G. Parisi, and J.J. Ruiz-Lorenzo *Phys. Rev. B* **58** 2740 (1998), P.-E. Berche, C. Chatelain, B. Berche and W. Janke *Eur. Phys. J. B* **38** 463 (2004), A.K. Murtazaev, I.K. Kamilov, and A. B. Babaev *Journal of Experimental and Theoretical Physics* **99** 1201 (2004), M. Hasenbusch,

TABLE XI. Critical exponent  $1/\nu^*$  extrapolated from the Finite-Size Scaling of the quantity  $X_1$  at the self-dual point  $\beta_c = 1$ .

$y$	0	0.25	0.5	0.75	1	1.25	Uncorr. Dis.
$q = 2, r = 2$	1.88(5)	1.87(6)	1.85(6)	1.82(5)	1.77(6)	1.70(7)	1.00(7)
$q = 2, r = 3$	1.88(4)	1.87(4)	1.84(4)	1.82(4)	1.76(5)	1.68(6)	0.97(10)
$q = 4, r = 4$	1.88(3)	1.86(3)	1.84(3)	1.80(3)	1.75(3)	1.66(4)	1.08(10)
$q = 8, r = 6$	1.88(3)	1.86(3)	1.84(3)	1.81(3)	1.75(3)	1.66(4)	1.10(10)
$q = 8, r = 7.5$	1.88(2)	1.87(2)	1.84(2)	1.80(3)	1.75(3)	1.66(4)	1.09(10)
$q = 8, r = 9$	1.88(2)	1.87(3)	1.84(3)	1.80(3)	1.75(3)	1.67(4)	1.08(10)
$q = 16, r = 10$	1.87(3)	1.86(2)	1.84(2)	1.80(3)	1.75(3)	1.66(3)	1.09(10)
$d - a/2$	1.875	1.857	1.835	1.8	1.75	1.667	1

TABLE XII. Critical exponent  $1/\nu^*$  extrapolated from the Finite-Size Scaling of the quantity  $X_1$  at different temperatures in the Griffiths phase.

$y$	0	0.25	0.5	0.75	1	1.25
$q = 2, \beta = 1$	1.88(4)	1.87(4)	1.84(4)	1.82(4)	1.76(5)	1.68(6)
$q = 2, \beta = 1.2$	1.91(4)	1.90(4)	1.86(5)	1.82(5)	1.79(5)	1.61(7)
$q = 8, \beta = 0.75$	1.86(3)	1.86(2)	1.83(3)	1.80(2)	1.74(3)	1.66(3)
$q = 8, \beta = 1$	1.88(2)	1.87(2)	1.84(2)	1.80(3)	1.75(3)	1.66(4)
$q = 8, \beta = 1.5$	1.89(3)	1.88(3)	1.85(3)	1.82(3)	1.76(3)	1.67(4)
$q = 8, \beta = 2$	1.89(3)	1.88(3)	1.86(3)	1.82(3)	1.77(4)	1.60(5)

- F. Parisen Toldin, A. Pelissetto, and E. Vicari, *J. Stat. Mech.* **P02016** (2007).
- [6] Y. Imry and M. Wortis *Phys. Rev. B* **19** 3580 (1979).
- [7] K. Hui and A.N. Berker *Phys. Rev. Lett.* **62** 2507 (1989); K. Hui and A.N. Berker *Phys. Rev. Lett.* **63** 2433 (1989).
- [8] M. Aizenman and J. Wehr *Phys. Rev. Lett.* **62** 2503 (1989); M. Aizenman and J. Wehr *Comm. Math. Phys.* **130** 489 (1990).
- [9] S. Chen, A.M. Ferrenberg and D. P. Landau *Phys. Rev. Lett.* **69** 1213 (1992); S. Chen, A.M. Ferrenberg, and D. P. Landau *Phys. Rev. E* **52** 1377 (1995).
- [10] C. Chatelain, and B. Berche *Phys. Rev. Lett.* **80** 1670 (1998). T. Olson, and A.P. Young *Phys. Rev. B* **60** 3428 (1999), C. Chatelain, and B. Berche *Phys. Rev. E* **60** 3853 (1999), J.L. Jacobsen, and M. Picco *Phys. Rev. E* **61** R13 (2000).
- [11] H. G. Ballesteros, L. A. Fernández, V. Martín-Mayor, A. Muñoz Sudupe, G. Parisi, and J. J. Ruiz-Lorenzo *Phys. Rev. B* **61** 3215 (2000)
- [12] C. Chatelain, B. Berche, W. Janke, and P.-E. Berche *Phys. Rev. E* **64** 036120 (2001), C. Chatelain, B. Berche, W. Janke, and P.-E. Berche *Nucl. Phys. B* **719** 275 (2005).
- [13] M.T. Mercaldo, J.-Ch. Anglès d'Auriac, and F. Iglói *Europhys. Lett.* **70** 733 (2005), M.T. Mercaldo, J.-Ch. Anglès d'Auriac, and F. Iglói *Phys. Rev. E* **73** 026126 (2006).
- [14] A. Weinrib, and B.I. Halperin *Phys. Rev. B* **27** 413 (1983).
- [15] J. Honkonen, and M.Y. Nalimov *J. Phys. A* **22** 751 (1989).
- [16] H. G. Ballesteros, and G. Parisi *Phys. Rev. B* **60** 12912 (1999), D. Ivaneyko, B. Berche, Y. Holovatch, and J. Ilnytskyi *Physica A* **387** 4497 (2008).
- [17] M.A. Rajabpour and R. Sepehrnia *J. Stat. Phys.* **130** 815 (2008).
- [18] R. Sknepnek and T. Vojta *Phys. Rev. B* **69**, 174410 (2004).
- [19] B.M. McCoy and T.T. Wu *Phys. Rev.* **176** 631 (1968); B.M. McCoy and T.T. Wu *Phys. Rev.* **188** 982 (1969).
- [20] D.S. Fisher *Phys. Rev. B* **51** 6411 (1995).
- [21] H. Rieger and F. Iglói *Phys. Rev. Lett.* **83**, 3741 (1999)
- [22] F.A. Bagaméry, L. Turban, and F. Iglói *Phys. Rev. B* **72** 094202 (2005).
- [23] J-Ch. Anglès d'Auriac and F. Iglói *Phys. Rev. Lett.* **90** 190601 (2003); M.T. Mercaldo, J-Ch. Anglès d'Auriac and F. Iglói *Phys. Rev. E* **69** 056112 (2004).
- [24] R.B. Griffiths *Phys. Rev. Lett.* **23**, 17 (1969)
- [25] T. Vojta *J. Phys. A* **39**, R143 (2006)
- [26] T. Senthil and S.N. Majumdar *Phys. Rev. Lett.* **76** 3001 (1996).
- [27] E. Carlon, C. Chatelain and B. Berche *Phys. Rev. B* **60** 12974 (1999).
- [28] P.-E. Berche, C. Chatelain and B. Berche *Phys. Rev. Lett.* **80** 297 (1998), C. Chatelain, P.-E. Berche, and B. Berche *Eur. Phys. J. B* **7** 439 (1999), D. Girardi, and N.S. Branco *Phys. Rev. E* **83** 061127 (2011).
- [29] C. Chatelain *Eur. Phys. Lett.* **102** 66007 (2013).
- [30] R. B. Potts *Math. Proc. Camb. Phil. Soc.* **48** 106 (1952), F. Y. Wu *Rev. Mod. Phys.* **54** 235 (1982), F. Y. Wu *Rev. Mod. Phys.* **55** 315 (1982).
- [31] C.M. Fortuin, and P.W. Kasteleyn *Physica* **57** 536 (1972).
- [32] A. Aharony, A.B. Harris, and S. Wiseman *Phys. Rev. Lett.* **81** 252 (1998).
- [33] W. Kinzel and E. Domany *Phys. Rev. B* **23** 3421 (1981).
- [34] R.H. Swendsen, and J.S. Wang *Phys. Rev. Lett.* **58** 86 (1987).

- [35] J. Ashkin et E. Teller *Phys. Rev.* **64** 178 (1943), C. Fan (1972) *Phys. Lett. A* **39** 136.
- [36] C. Fan *Phys. Rev. B* **6** 902 (1972).
- [37] L. P. Kadanoff *Phys. Rev. Lett.* **39** 903 (1977), L. P. Kadanoff, and A. C. Brown *Annals of Physics* **121** 318 (1979).
- [38] S. Wiseman, and E. Domany *Phys. Rev. E* **48** 4080 (1993), J. Salas and A.D. Sokal *J. Stat. Phys.* **85** 297 (1996).
- [39] S. Wiseman, and E. Domany *Phys. Rev. E* **52** 3469 (1995).
- [40] A. Aharony and A.B. Harris *Phys. Rev. Lett.* **77**, 3700 (1996).
- [41] M. Hasenbusch, F. Parisen Toldin, A. Pelissetto, and E. Vicari, *Phys. Rev. E* **78**, 011110 (2008)
- [42] C. Chatelain, B. Berche, and L.N. Shchur *J. Phys. A* **34** 9593 (2001).
- [43] Errors on the derivative  $\frac{d}{d\beta} \ln \overline{\langle m \rangle}$  were considerably improved compared to Ref. [29]. As discussed in the latter reference, this derivative is computed as the difference of two observables,  $\overline{\langle me \rangle}$  and  $\overline{\langle m \rangle \langle e \rangle}$ , which are several orders of magnitude larger than their difference. If these two observables are computed separately, as it was the case in Ref. [29], it is natural to estimate the error on their difference as the sum of their respective errors. However, this does not reflect the true error on the difference  $\bar{X} = \overline{\langle me \rangle} - \overline{\langle m \rangle \langle e \rangle}$  because the two are correlated. The difference was therefore computed during the simulation and the error, estimated by  $\sqrt{(\bar{X}^2 - \overline{X^2})/N}$  where  $N$  is the number of disorder configuration.
- [44] The large estimates of the exponent  $\nu$  given in the text contrast with the values of this exponent for the (uncorrelated) random Potts models, known to be close to 1. However, large exponents  $\nu$  are frequent. In some cases, the correlation length exponent even goes to infinity, which means that the correlation length grows exponentially fast as the critical temperature is approached. It is the case of the 1D Ising model for which  $\xi \sim e^{2/T}$  and of the anti-ferromagnetic Ising model on a triangular lattice. In the neighborhood of a Kosterlitz-Thouless phase transition, like in the 2D XY model for example, the correlation length behaves as  $\xi \sim e^{at-\sigma}$  where  $t = T - T_{KT}$ . An algebraic growth with an exponent  $\nu \simeq 10 - 40$  is therefore not a particularly fast growth. Moreover, note that the Weinrib-Halperin prediction  $\nu = 2/a$  gives also large values (between 3 and 8) for the disorder correlations considered. Finally, note that, as commented at the beginning of Sec. IV, the exponent  $\nu$  is defined only through Finite-Size Scaling so a scaling law such as  $\xi \sim t^{-\nu}$  may not be applicable in the Griffiths phase if the correlation length  $\xi$  diverges at any temperature in this region.
- [45] M. Schwartz, and A. Soffer *Phys. Rev. Lett.* **55** 2499 (1985).
- [46] A.J. Bray, and M.A. Moore *J. Phys. C* **18** L927 (1985).
- [47] In the context of the 3D RFIM, the susceptibility  $\chi_1$  was also shown to diverge at the critical point with a different exponent than the average susceptibility [46]. Different notations were introduced. The correspondence with our notation is  $(\gamma/\nu)^* = 4 - \bar{\eta}$ .
- [48] The regular part of the energy density is responsible for the fact that the latter is a self-averaging quantity. According to the Finite-Size Scaling behaviors discussed in the text, the ratio  $R_e$  decays algebraically with the lattice size:

$$R_e = \frac{\overline{\langle e \rangle^2} - \overline{\langle e \rangle}^2}{\overline{\langle e \rangle}^2} = \beta^2 \frac{C_2/L^d}{\overline{\langle e \rangle}^2} \sim L^{(\alpha/\nu)^* - d} \quad (28)$$

since  $(\alpha/\nu)^* < d$  and  $\overline{\langle e \rangle} \sim L^0$ . In the magnetic sector,  $R_m = \frac{\chi_2/L^d}{\overline{\langle m \rangle}^2}$ . In contrast to  $\overline{\langle e \rangle}^2$ , the denominator is singular and scales as  $L^{-2\beta/\nu}$ . Because  $\chi_2 \sim L^{(\gamma/\nu)^*}$  where  $(\gamma/\nu)^*$  satisfies the hyperscaling relation,  $R_m$  scales as  $L^0$ , which allows for a non-vanishing limit and therefore a possible absence of self-averaging.